HHS Public Access

Author manuscript

Acc Chem Res. Author manuscript; available in PMC 2024 August 15.

Published in final edited form as:

Acc Chem Res. 2023 August 15; 56(16): 2197–2212. doi:10.1021/acs.accounts.3c00297.

Ligand–Copper(I) Primary O_2-Adducts: Design, Characterization, and Biological Significance of Cupric–Superoxides

Bohee Kim,

Department of Chemistry, The Johns Hopkins University, Baltimore, Maryland 21218, United States

Kenneth D. Karlin

Department of Chemistry, The Johns Hopkins University, Baltimore, Maryland 21218, United States

CONSPECTUS:

In this Account, we overview and highlight synthetic bioinorganic chemistry focused on initial adducts formed from the reaction of reduced ligand–copper(I) coordination complexes with molecular oxygen, reactions that produce ligand–$Cu^{II}(O_2^{\bullet-})$ complexes ($O_2^{\bullet-} \equiv$ superoxide anion). We provide mostly a historical perspective, starting in the Karlin research group in the 1980s, emphasizing the ligand design and ligand effects, structure, and spectroscopy of these O_2 adducts and subsequent further reactivity with substrates, including the interaction with a second ligand–Cu^I complex to form binuclear species. The Account emphasizes the approach, evolution, and results obtained in the Karlin group, a synthetic bioinorganic research program inspired by the state of knowledge and insights obtained on enzymes possessing copper ion active sites which process molecular oxygen. These constitute an important biochemistry for all levels/types of organisms, bacteria, fungi, insects, and mammals, including humans.

Copper is earth abundant, and its redox properties in complexes allow for facile Cu^{III}/Cu^I interconversions. Simple salts or coordination complexes have been well known to serve as oxidants for the stoichiometric or catalytic oxidation or oxygenation (i.e., O-atom insertion) of organic substrates. Thus, copper dioxygen- or peroxide-centered synthetic bioinorganic studies provide strong relevance and potential application to synthesis or even the development of cathodic catalysts for dioxygen reduction to hydrogen peroxide or water, as in fuel cells. The Karlin group's focus however was primarily oriented toward bioinorganic chemistry with the goal to provide fundamental insights into the nature of copper–dioxygen adducts and further reduced and/or protonated derivatives, species likely occurring in enzyme turnover or related in one or more aspects of formation, structure, spectroscopic properties, and scope of reactivity toward organic/biochemical substrates.

Prior to this time, the 1980s, O_2 adducts of redox-active first-row transition-metal ions focused on iron, such as the porphyrinate–Fe centers occurring in the oxygen carrier proteins myoglobin and

Corresponding Author: **Kenneth D. Karlin** – *Department of Chemistry, The Johns Hopkins University, Baltimore, Maryland 21218, United States;* karlin@jhu.edu.

Complete contact information is available at: https://pubs.acs.org/10.1021/acs.accounts.3c00297

The authors declare no competing financial interest.

hemoglobin and that determined to occur in cytochrome P-450 monooxygenase turnover. Deoxy (i.e., reduced Fe(II)) heme proteins react with O_2, giving Fe^{III}–superoxo complexes (preferably referred to by traditional biochemists as ferrous–oxy species). And, it was in the 1970s that great strides were made by synthetic chemists in generating hemes capable of forming O_2 adducts, their physiochemical characterization providing critical insights to enzyme (bio)chemistry and providing ideas and important goals leading to countless person years of future research.

Graphical Abstract

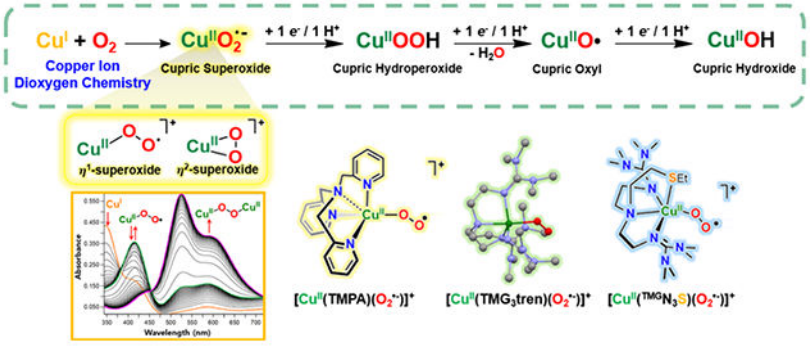

1. INTRODUCTION

Dioxygen reducing processes lie at the center of biological and societal/industrial energy requirements; they include cellular respiration[4] and metal-ion-mediated reactions utilizing O_2.[5] Aqueous environment reduction (Figure 1) includes stepwise electron–proton transfers involving overall 4-electron–proton transformation of O_2 to H_2O. One-electron addition to dioxygen is a slightly uphill process, yielding superoxide radical anion ($O_2^{\bullet-}$). H_2O_2 is afforded by the further one-electron two-proton reduction. Peroxide O–O reductive cleavage is critically important in chemistry–biology; homolysis gives hydroxyl radical, a powerful indiscriminate oxidant.[6]

With a research focus on copper(I)–O_2 chemistry[5a,7] relevant to copper enzymes[8] activating O_2 for oxidation–oxygenation reactions, the copper ion is an electron donor (Cu^I) or Lewis acid (Cu^{2+}; instead of H^+) and facilitates O_2 reduction–protonation by coordination to O_2-derived fragments (Figure 1). Protein– or ligand–Cu^I/O_2 reactivity gives Cu^{II}–superoxide species.[8,9] Supplementation by one e^-/H^+ gives copper(II)–hydroperoxide species. A Cu^{II}–oxyl[10] is a copper-ligated deprotonated hydroxyl radical Cu^{II}–$O^{\bullet}$ formed via peroxide O–O bond cleavage and reduction–protonation (Figure 1). Further addition of a e^-/H^+ yields a copper(II)–hydroxo species which may act (i) as a substrate oxidant/proton acceptor or (ii) via rebound, $Cu^{II}OH + R^{\bullet} \rightarrow Cu^I + ROH$.[11] Elucidation of the (bio)chemistry of copper–oxygen fragments and their transformations or interconversions is the goal of multiple research communities. How are $Cu^{II}(O_2^{\bullet-})$, $Cu^{II}OOH$, and $Cu^{II}O^{\bullet}$ formed, what are their structures/physical/spectroscopic and bonding properties, how are they related by redox/proton transfer, and what is their substrate reactivity? Many copper enzymes possess active sites with two, three, or even four Cu's in proximity; thus, the nature of O_2-derived

fragments bound to 2–4 copper ions expands the landscape of interest and importance. Figure 1 illustrates known Cu_2O_2 structures.[7]

2. COPPER(II)–SUPEROXIDES IN METALLOENZYMES

As this Account focuses on copper(II)–superoxides, we indicate how such species pervade copper biochemistry, participating in key hydrogen-atom abstractions (HAA) (Figure 2). In the monooxygenase catalytic cycle,[5b] initial Cu^I/O_2 reactivity gives the cupric–superoxide. Further reductive steps would lead to a Cu^{II}–oxyl or localized hydroxyl radical (Figure 1), oxidants powerful enough to attack the very strong substrate C–H bonds. Peptidylglycine α-hydroxylating monooxygenase (PHM) and dopamine β-monooxygenases (DβM) are ascorbate-dependent enzymes involved in hormone/neurotransmitter biosynthesis,[8,12] referred to as “noncoupled” binuclear enzymes. Biochemical, structural, spectroscopic, and computational investigations have shown that Cu_M (Figure 2), with its two histidine imidazolyl plus methionine thioether ligands, undergoes Cu_M^I–O_2 reactivity, giving a Cu^{II}_M–superoxide (with an X-ray structure determined)[12a] which initiates catalysis via substrate HAA. Lytic polysaccharide monooxygenases (LPMOs)[13] and *particulate*-methane monooxygenase (*p*MMO),[14] both possessing a “histidine brace” (imidazolyl and chelating amine terminus),[13b] effect polysaccharide oxidative breakdown or methane to methanol conversion, respectively; their (bio)chemistries are critical in energy conversion. The formylglycine generating enzyme (FGE)[15] features a copper(I) bis-cysteinate which when further ligated by a substrate cysteine reacts with O_2, giving a Cu^{II}–superoxide which attacks the methylene group via HAA; further steps lead to products C_α-formylglycine and H_2S(g).

Galactose oxidases (GOs)[16] (Figures 2 and 3) and amine oxidases (AOs)[16] effect two-electron substrate oxidations, producing H_2O_2. Their active sites bear post-translationally modified amino acid cofactors, a cross-linked Tyr–Cys for GO (Figure 3). In normal turnover, a Cu^{II}–superoxide abstracts an H atom from the Tyr–Cys group, generating a ligated Cu^{II}–phenoxyl radical intermediate, ready to effect substrate HAA, providing for overall RCH_2OH to RC(O)H conversion.[8]

Cytosolic Cu–Zn superoxide dismutases (SOD1’s)[17] detoxify superoxide by disproportionation. With active site copper(II), a central imidazolate bridges the copper and structural zinc ions. Cu^{II}–SOD plus $O_2^{\bullet-}$ effects copper(II) reduction and O_2(g) release. The Cu^I produced is now three coordinate; the bridging imidazolate has been protonated and only binds zinc(II). Reaction of a second superoxide substrate with the His_3–copper(I) leads to H_2O_2, regenerating copper(II) (Figure 4a).

Mitochondrial cytochrome *c* oxidase (C*c*O)[4,18] catalyzes the $4e^-/4H^+$ reduction of O_2 to two waters, coupling this downhill reaction to membrane proton translocation and ATP biosynthesis. A transient Cu^{II}–superoxide intermediate forms during turnover (Figure 4b).

3. N_4 TETRADENTATE LIGANDS

The extensive copper(I)/O_2 biochemistry highlights the reasons for fundamental investigations relating to cupric–superoxo species including when a Cu^{II}–superoxide

reacts with a substrate or undergoes reduction–protonation (Figure 1). When this PI started research, no synthetic chemistry Cu^{I}–O_2 adducts or derived species existed. A copper–protein X-ray structure was a “blue” Type-1 electron transfer protein, plastocyanin.[19] “Blue” multicopper oxidases possessed a biochemistry–biophysics (UV–vis and EPR spectroscopies; electron transfer investigations).[20] For hemocyanins (dicopper O_2 carriers in arthropods and mollusks with $Cu^{I}(His)_3$ ligation) and tyrosinases (dicopper monooxygenases; *o*-phenol hydroxylation, melanin biosynthesis),[8] deeply colored O_2 adducts were known, later identified (X-ray)[21] as $(His)_3Cu^{II}$–$(\mu\text{-}\eta^2\text{:}\eta^2\text{-}O_2^{2-})$–$Cu^{II}(His)_3$ species (Figure 1).

While we and others designed binucleating ligands toward modeling dicopper proteins,[7] we also strived to elucidate simpler fundamentals, where one ligand–copper(I) entity reacted with dioxygen. One investigative track utilized tripodal tetradentate ligands (Figure 5).[9a,22] Important considerations were as follows.

- **a.** Ligand–copper(I) complex O_2 binding would involve partial or full electron transfer; an O_2 adduct would be a Cu^{II} complex with bound superoxide radical–anion.
- **b.** N-donor ligands should be most suitable as they accommodate both copper(I) and copper(II). Histidyl imidazoles are ligands in hemocyanins, tyrosinases, multicopper oxidases, and Type-1 electron transfer proteins.
- **c.** Consideration of copper(I) vs copper(II) coordination preferences would be required. Copper(I) forms two-, three-, and four-coordinate (tetrahedral) complexes. Copper(II) prefers tetra- (planar) or pentacoordination. Ligand–$Cu^{II/I}$ redox relationships[23] revealed that three-coordinate copper(I) exhibits positive reduction $E°/E_{1/2}$ potentials (favoring Cu(I)). Tetradentate ligands which enforce planar copper coordination exhibit negative values.
- **d.** Zuberbühler’s kinetics investigations[24] led to hypotheses concerning suitable coordination in hemocyanins in order to facilitate reversible O_2 binding; 2–3 imdazolyl donors provide optimal copper(I) coordination, while O_2 addition would bestow a not too “cupric-like” $(N_2/N_3)Cu^{II}$–(O_2^{2-})–$Cu^{II}(N_2/N_3)$ adduct.

Tripodal tetradentate ligands were in part chosen because neither Cu(I) nor Cu(II) complexes would be able to form planar coordination environments; copper(I) salts or complexes may readily disproportionate if the surrounding ligand favors copper(II). The ligands in Figure 5 vary systematically in chelate ring size (TMPA, 5-membered rings; TEPA, 6-membered rings). Rorabacher’s[25] broad studies of ligands of varying denticity, chelate ring size, and donor atom type showed that ligand–copper$^{II/I}$ reduction potentials depended on the ligand binding K_{eq} to copper(II) and not copper(I); six-membered chelate rings favor copper(I), while copper(II) prefers five-membered chelate rings. For copper complexes with TMPA through TEPA (Figure 5), an ~0.5 V variation in ligand–copper$^{II/I}$ $E_{1/2}$ value was observed.

3.1. N_4 Pyridylalkylamine Ligands

The copper(I) complex with TEPA ligand was unreactive toward O_2; by contrast, $[Cu^{I}(tmpa)(MeCN)]^{+}$ is extremely O_2 sensitive. We successfully crystallized the first known copper–

dioxygen adduct, the *trans*-μ1,2-peroxodicopper(II) complex $[\{Cu^{II}(tmpa)\}_2(O_2^{2-})]^{2+}$ (Figure 6).[26] Important insights were obtained utilizing UV–vis-monitored low-temperature stopped-flow kinetics.[1,27] An intermediate, later proven to be $[Cu^{II}(tmpa)(O_2^{\bullet-})]^+$, forms in milliseconds (Figures 6 and 7).

Nitriles are excellent Cu^I ligands; the propionitrile solvent inhibits O_2 binding. We were able to devise "flash-and-trap" experiments on $[Cu^I(tmpa)(CO)]^+$ in the presence of O_2 in tetrahydrofuran (noncoordinating). The binding of O_2 approaches the diffusion limit, k_{on} = 1.3×10^9 M^{-1} s^{-1} (RT);[18,28] k_{on} is greater than that known for other ligand–Cu^I complexes and even heme proteins (Figure 7), pointing to the biological and/or chemical synthetic utility of copper in redox processes. These findings are explained as related to the imposed geometry and electronic structure for a ligand–metal system.[18,27b]

The O_2 reduction reaction (ORR) is of contemporary importance in energy considerations and application to fuel-cell cathodic catalysis. Both $2e^-/2H^+$ (to H_2O_2) and $4e^-/4H^+$ (to $2H_2O$) reductions are important, and selectivity is a research goal. Interestingly, $[Cu^I(tmpa)]^+$ catalyzes O_2 reduction to water in the presence of decamethylferrocene (Fc*) and $HClO_4$ in acetone.[29] Mechanistic studies reveal $[Cu^{II}(tmpa)(O_2^{\bullet-})]^+$ formation followed by the appearance of $[\{Cu^{II}(tmpa)\}_2(O_2^{2-})]^{2+}$, which is further reduced/protonated to give water and not H_2O_2.[29a] By replacing $HClO_4$ with $Sc(OTf)_3$, a two-electron reduction instead occurs. $[Cu^I(tmpa)]^+/O_2$ reactivity gives $[Cu^{II}(tmpa)(O_2^{\bullet-})]^+$, which undergoes fast reduction and trapping of peroxide dianion by Sc^{3+} ; no "dimerization" giving $[\{Cu^{II}(tmpa)\}_2(O_2^{2-})]^{2+}$ occurs (Figure 8).[29b] In contrast, quinolyl ligands confer a very positive reduction potential for $[Cu^{II/I}(BzQ)]^+$; now, weaker reductants (Me_2Fc or Fc, compared to Fc*) promote O_2 activation and two-electron ORR (Figure 8).[29b]

Tetradentate ligands with quinolyl rather than pyridyl "arms" were also generated (Chart 1; Figure 9) to probe resultant copper complex steric and/or electronic effects. For ligand–Cu^I complexes, TMQA confers a more positive $Cu^{II/I}$ $E_{1/2}$ by 370 mV.[27a] Dramatic differences in O_2 reactivity are also observed. No 1:1 Cu^{II}–$(O_2^{\bullet-})$ complex could be observed in the $[Cu^I(bpqa)]^+/O_2$ reaction; only the peroxo–dicopper(II) complex analog $[\{Cu^{II}(bpqa)\}_2(O_2^{2-})]^{2+}$ forms. For BQPA, a differing scenario occurs.

In ca. 1 s at −80 °C, the *trans*-peroxo complex forms, but this slowly isomerizes to a bis-μ-oxo–dicopper(III) complex, λ_{max} = 380 nm, a close analogue to that complex discovered and characterized by Suzuki using Me_2tpa (with two 6-methylpyridyl rather than quinolyl arms).[30] Here, O_2 can be recovered from the bis-μ-oxo–dicopper(III) complex, indicating that the BQPA chemistry steps shown (Figure 9) are reversible. Ligand 2-quinolyl steric effects make $[Cu^I(tmqa)]^+$ unreactive toward O_2.

Scheme 1 most generally applies to $[Cu^I(ligand)]^+/O_2$ reactivity. Thermodynamic stabilization drives $[Cu^{II}(ligand)\text{-}(O_2^{\bullet-})]^+$ to react with a second Cu^I species, giving binuclear peroxo–dicopper(II) products. However, we could cryogenically stabilize the cupric–superoxo species by utilizing TMPA derivatives employing strong donor groups in the pyridyl para position. Kinetic/thermodynamic studies using ^{DMM}TMPA or ^{DMA}TMPA (Chart 1) show that k_{O2} increases and k_{-O2} decreases (thus, K_{O2} (= k_{O2}/k_{-O2}) increases) (i)

consistent with oxygenation being accompanied by electron transfer from copper(I) to O_2 (giving superoxide anion) and (ii) large K_{O2} values suppress binuclear peroxo–dicopper(II) formation, because the ligand–Cu^I concentration present decreases. In fact, benchtop handling of ligand–Cu^I/O_2 solutions with these two ligands provides for almost exclusive stabilization of $[Cu^{II}(ligand)(O_2^{\bullet-})]^+$ species ($t_{1/2} \geq 4$ h, −85 °C for ^{DMA}tmpa).[27b,31]

Such stabilization allowed for in-depth characterization and insightful comparisons. For $[Cu^I(tmpa)]^+$ vs $[Cu^I(^{DMA}tmpa)]^+$, $E_{1/2}$ for the latter is 300 mV more positive; for $[Cu^I(tmpa)\text{-}(CO)]^+$ vs $[Cu^I(^{DMA}tmpa)(CO)]^+$, ν(CO) values are 2092 and 2079 cm^{-1}.[27b] Thus, $[Cu^I(^{DMA}tmpa)]^+$ is a much better electron donor than is $[Cu^I(tmpa)]^+$. $[Cu^{II}(^{DMA}tmpa)(O_2^{\bullet-})]^+$ is a brilliant green color in solution, exhibiting multiple UV–vis absorptions, and it is EPR silent. In resonance Raman (rRaman) spectroscopy, ν(O–O) = 1121 cm^{-1}, shifted to 1058 cm^{-1} for $^{18}O_2$. Further analysis of rRaman spectra of $[Cu^{II}(^{DMA}tmpa)(O_2^{\bullet-})]^+$ using gas mixtures with ^{16}O–^{18}O (Figure 10) revealed that the O atoms of the superoxo fragment in this (and these complexes with tripodal tetradentate ligands) are chemically inequivalent, thus consistent with possessing an end-on geometry, with only one O atom binding to the copper(II) ion.[31a] This is as we depicted in our 1993 kinetic study (Figures 7 and 8) and corroborated by the X-ray structure from Schindler and co-workers[32] using the TMG_3tren ligand (Chart 2; also discussed below). Roth, using low-temperature NMR spectroscopy,[33] followed by a detailed MCD spectroscopic and computational investigation from Solomon and co-workers[34] provided electronic structural and bonding characterization of such end-on-bound copper(II)–superoxo complexes. They possess $S = 1$ ground-state structures; the copper(II) ion and superoxide ligand unpaired electrons are ferromagnetically coupled.

The stability of $[Cu^{II}(^{DMA}tmpa)(O_2^{\bullet-})]^+$ allowed for first time reactivity studies. Addition of *p*-MeO-2,6-di-*tert*-butyl-phenol (*p*-MeO-2,6-DTBP) yielded *p*-MeO-2,6-di-*tert*-butyl-phenoxyl radical (UV–vis 405 nm peak; EPR $g \approx 2$ signal) via HAA. Reaction with *p*-X-2,6-DTBP (X = $-^t$Bu, −H) gave 2,6-di-*tert*-butyl-1,4-benzoquinone products, arising from further reaction of the phenoxyl radical with a second equivalent of $[Cu^{II}(^{DMA}tmpa)(O_2^{\bullet-})]^+$.[31a] $[Cu^{II}(^{DMM}tmpa)(O_2^{\bullet-})]^+$ was utilized in a more detailed mechanistic study for oxidation of various *p*-X-2,6-DTBP's. The deuterium kinetic isotope effects (KIEs) determined were consistent with the conclusion that phenol oxidations proceeded via HAA. Further insights were derived from correlations of the reaction rate constants between the cumyl peroxyl radical toward the same phenols; HAA is rate determining, but these reactions occur via "partial" concerted electron and proton transfer.[31b]

To generate highly thermally stable copper(II)–superoxo complexes, England and co-workers[35] introduced bulky *meta*-aryl-substituted TMPA's (Ar = tpb, dpb, or dtbpb; Chart 1), The $[Cu^I(^{Ar3}tmpa)]^+$ complexes were characterized by cyclic voltammetry (CV); the bulky substituents do not meaningfully influence the pyridyl group's donor ability. $[Cu^I(^{Ar3}tmpa)]^+$ solutions in tetrahydrofuran at −80 °C bubbled with O_2(g) afforded green superoxo complexes; characterization was derived from UV–vis, rRaman, and NMR spectroscopies and magnetic measurements. These confirmed the superoxide end-on binding and complex $S = 1$ ground states. The particular stability of $[Cu^{II}(^{tpb3}tmpa)(O_2^{\bullet-})]^+$ permitted further substrate reactivity investigations. Oxidation of O–H (phenols), N–H (e.g.,

hydrazines), and C–H bonds containing substrates occurred via HAA, as corroborated with the observation of large KIEs.

Karlin and Hoffman[36] recently reported an EPR and ENDOR spectroscopic interrogation of (frozen) solutions of, for example, $[Cu^{II}(^{DMM}tmpa)(O_2^{\bullet-})]^+$ (Figure 11). By cryoreduction (γ-irradiation) and protonation by annealing (i.e., warming), electron transfer and/or protonation interrelationships could be established. Cryoreduction of $[Cu^{II}(^{DMM}tmpa)(O_2^{\bullet-})]^+$ resulted in initial electron transfer to the copper(II) ion, yielding a new molecular type, a copper(I)–superoxo species. Internal electron transfer followed, giving a copper(II)–peroxide, which when warming picked up a proton to give $[Cu^{II}(^{DMM}tmpa)(OOH)]^+$.

3.2. Hydrogen-Bonded Cupric–Superoxide Complexes

In coordination or organometallic chemistry, there has been considerable interest in utilization of multidentate ligands with built-in hydrogen-bonding functionalities. In fact, Masuda and co-workers[37] utilized TMPA derivatives with 2-pyridylamino or pivalamido substituents to study the effects of these input H-bonding groups on the chemistry/spectroscopy of copper(II)–azido or peroxodicopper(II) complexes. We chose to examine these or related ligands to learn about their influences on copper(II)–superoxo complexes.

By adopting amino (NH_2), pivalamido (PV), or penta-fluorobenzylamine (F_5BA) groups at the 2 position of one or more of the pyridyl arms (Chart 1), ligand–copper(I) precursor oxygenations led to cryogenically (−135 °C; 2-methyltetrahydroluran (MeTHF)) stabilized $[Cu^{II}(^{F5BA}tmpa)\text{-}(O_2^{\bullet-})]^+$ and $[Cu^{II}(^{1PV}tmpa)(O_2^{\bullet-})]^+$ complexes.[38] Studies with azido complexes of these ligands, N_3^- being a good spectroscopic surrogate for superoxide or (hydro)peroxide anions,[2,38a] revealed that significant H bonding occurs between the PV (or $-NH_2$) ligand group (Chart 1) and the proximal (to copper) N atom (in azide) or O atom (in superoxide). Studies with azido complexes indicated the relative strength of H bonding with the varying ligands employed (Figure 12 and Chart 1); an upshift in the multiply bonded N–N stretch (due to a change in azido resonance form preferred) occurs with stronger H bonding to the proximal N atom,[38a] Figure 12.

Oxidative reactions of *p*-MeO-2,6-DTBP with $[Cu^{II}(^{F5BA}tmpa)(O_2^{\bullet-})]^+$ and $[Cu^{II}(^{1PV}tmpa)(O_2^{\bullet-})]^+$ were carried out. The results revealed that H bonding results in a higher efficiency in HAA reactivity ($k = 3.1 \times 10^{-1}$ M^{-1} s^{-1} ($[Cu^{II}(tmpa)(O_2^{\bullet-})]^+$), 11.5×10^{-1} M^{-1} s^{-1} ($[Cu^{II}(^{F5BA}tmpa)(O_2^{\bullet-})]^+$), and 9.9×10^{-1} M^{-1} s^{-1} ($[Cu^{II}(^{1PV}tmpa)(O_2^{\bullet-})]^+$)).

In another study,[2] the physical properties and reactivities of $[Cu^{II}(^{NH2}tmpa)(O_2^{\bullet-})]^+$, $[Cu^{II}(^{(NH2)2}tmpa)(O_2^{\bullet-})]^+$, and $[Cu^{II}(^{1PV}tmpa)(O_2^{\bullet-})]^+$ vs $[Cu^{II}(^{2PV}tmpa)(O_2^{\bullet-})]^+$ (−135 °C, MeTHF), now stable to conversion to *trans*-peroxo–dicopper(II) analogues, were surveyed. For this series, a strong charge transfer band in the 400–420 nm range underwent a blue shift with increased H-bonding capability. In rRaman spectroscopy, the O–O stretching frequencies occurred over the range 1121–1130 cm^{-1}. HAA oxidations of phenols by $[Cu^{II}(^{R}tmpa)(O_2^{\bullet-})]^+$ were studied, all giving a phenoxyl radical plus hydroperoxo–copper(II) complexes $[Cu^{II}(^{R}tmpa)\text{-}(-OOH)]^+$ (Figure 13), i.e., superoxide plus an electron and proton gives hydroperoxide. The oxidative ability of the series was dramatically enhanced with an increase in strength and/or number of intramolecular

H-bonding groups (Figure 13). All four of the superoxo–copper(II) complexes could oxidize *p*-MeO-2,6-DTBP with a weak O–H bond (bond dissociation energy (BDE) = 80.8 kcal/mol). $[Cu^{II}(tmpa)(O_2^{\bullet-})]^+$ and $[Cu^{II}(^{NH2}tmpa)(O_2^{\bullet-})]^+$ were unable to react with *p*-methoxyphenol as substrate, However, $[Cu^{II}(^{1PV}tmpa)\text{-}(O_2^{\bullet-})]^+$, $[Cu^{II}(^{(NH2)2}tmpa)(O_2^{\bullet-})]^+$, and $[Cu^{II}(^{2PV}tmpa)\text{-}(O_2^{\bullet-})]^+$ could effect these HAA reactions, k = 0.02, 0.04, and 0.21 M^{-1} s^{-1}, respectively. Furthermore, $[Cu^{II}(^{2PV}tmpa)\text{-}(O_2^{\bullet-})]^+$ could oxidize *p*-cresol (O–H BDE = 91.5 kcal/mol) and also the C–H substrate 9,10-dihydroanthracene (BDE = 79.7 kcal/mol). Previously, we showed that $[Cu^{II}(^{1PV}tmpa)\text{-}(O_2^{\bullet-})]^+$ could effect an HAA reaction on the C–H bond in 1-benzyl-1,4-dihydronicotinamide (BDE = 70.7 kcal/mol).[38b]

As H bonding leads to more stabilized superoxo–copper(II) complexes, the greater the K_{O2} value ($K_{O2} = k_{O2}/k_{-O2}$), leaving behind decreased concentrations of copper(I) precursors $[[Cu^{I}(^{R}tmpa)]^+]$, those needed to form peroxodicopper(II) complexes in the second step (Scheme 1). This is analogous the effect of H bonding to the superoxo moiety in hemoglobins, which decreases O_2 dissociation (k_{-O2}).[38a]

3.3. N_4 Tris(2-aminoethyl)amine (tren)-Type Ligands

Schindler, Sundermeyer, and co-workers[32,39] employed the very strongly donating ligand TMG_3tren. Its copper(I) complex reversibly binds O_2; dimerization to give a binuclear peroxo–dicopper(II) complex does not occur. $[Cu^{II}(TMG_3tren)(O_2^{\bullet-})]^+$, first formed in acetone at −70 °C, is the only crystallographically characterized end-on superoxo–copper(II) complex (Figure 14). The strong UV–vis bands at 442 and 690 nm closely match those for $[Cu^{II}(tmpa)(O_2^{\bullet-})]^+$ (Figure 6). The O–O stretching frequency of $[Cu^{II}(TMG_3tren)(O_2^{\bullet-})]^+$ was detected at 1122 and 1117 cm^{-1} by IR and rRaman spectroscopies, respectively. Also, it is an S = 1 complex. As for heme–O_2 adducts (porphyrinate–Fe^{III}–superoxides), dioxygen could be photoejected from $[Cu^{II}(TMG_3tren)(O_2^{\bullet-})]^+$ and $[Cu^{II}(^{1PV}tmpa)(O_2^{\bullet-})]^+$, the kinetics of O_2 recombination could be followed by transient absorption spectroscopy (Figure 14a and 14c), and very large rate constants were determined (Figure 7).[18]

We further utilized $[Cu^{II}(TMG_3tren)(O_2^{\bullet-})]^+$ for reduction/protonation studies,[40] as such e^-/H^+ chemistry pervades (bio)chemical O_2 activation (Figure 1). Fc* will not reduce $[Cu^{II}(TMG_3tren)(O_2^{\bullet-})]^+$. However, with trifluoroacetic acid ($HOAc_F$) added to form an adduct, $[Cu^{II}(TMG_3tren)(O_2^{\bullet-})\text{-}(HOAc_F)]^+$ (Figure 14d), reduction by Fc* or octamethylferrocene occurs (Fc* is 6.1× faster (−80 °C)); dimethylferrocene is unreactive. We could thus bracket this superoxide to hydroperoxide transformation as having +0.12 V < $E°'$ < +0.44 V vs SCE (in 2-methyltetrahydrofuran) (roughly from −0.4 to −0.1 V vs Fc^+/Fc). While measured at low temperature in organic solvents, such redox potentials can still have a meaning that can be appreciated as having biological implications. The agents cytochrome *c* and ascorbate in acetonitrile possess redox potentials lying between those of octamethylferrocene and dimethylferrocene.[41] Thus, a metal–ligand–(O_2^{n-}) species that undergoes reduction/(protonation) within the octamethylferrocene/dimethylferrocene "window" in organic solvents would be reduced if placed in biological media (such as in a metalloenzyme active site). In other works,[41] we demonstrated that a superoxide anion ligated as a bridging ligand in binuclear copper(II) complexes undergoes reduction (to

coordinated/bridged peroxide dianion) with roughly −0.6 V < $E°'$ < −0.3 V vs Fc^+/Fc (in organic solvents).

Schindler[42] and Suzuki[43] and co-workers were able to generate and study superoxo–copper(II) and/or peroxodicopper(II) complexes with amino-derivatized tren ligands. $[Cu^{II}(^{Me,Me}tren)(O_2^{\bullet-})]^+$ [42,43] (see also a kinetic study, Figure 7),[42] $[Cu^{II}(^{H,Bn}tren)(O_2^{\bullet-})]^+$, and $[Cu^{II}(^{Me,Bn}tren)\text{-}(O_2^{\bullet-})]^+$[43] were detected/characterized by UV–vis and rRaman spectroscopies exhibiting behavior very similar to TMPA derivatives; *trans*-peroxo–dicopper(II) analogs also form.[42,43] Itoh[44] designed/synthesized a tren ligand derivative having very bulky and hydrophobic HIPT substituents (Chart 3), stabilizing $[Cu^{II}(HIPT_3tren)(O_2^{\bullet-})]^+$ (end-on superoxo ligand, $S = 1$ ground state) in acetone at −90 °C.

Comba and co-workers[45] studied the oxygenation of copper(I) complexes with second-generation bispidine ligands ($L2^R$; Chart 3). Via spectroscopic and computational analyses, several O_2-derived species were observed under cryogenic conditions, including an end-on superoxo–copper(II) complex (λ_{max} = 402 and 664 nm).

Reinaud and co-workers[46] carried out investigations of copper(I)/O_2 chemistry utilizing elaborated tren-based Calixarene ligands. $[Cu^I(Calix[6]amido\text{-}tren)]^+/O_2$ (Chart 3) chemistry yielded an end-on cupric superoxide complex capable of a remarkable four-electron oxygenation of a ligand methylene group (giving a ketone). Overall, the Reinaud group's supramolecular chemistry studies led to many new insights into copper(I)/O_2 oxidative reactivity.

It is worth mentioning the superoxo–copper(II) complex early on reported by Valentine[47] using the N_4 macrocycle tet b (Chart 3). This EPR-silent species was generated via reaction of $[Cu^{II}(tet\ b)]^{2+}$ with KO_2/crown ether. Via low-temperature oxygenation of $[Cu^I(tet\ b)]^+$, Shindler[48] recently crystallized the peroxo–dicopper(II) analogue.

3.4. N_3S Tetradentate Ligands

Castillo[49] recently reviewed the coordination chemistry of copper with thioether ligands as relevant to the PHM and DβM enzyme Cu_M. The presence of this RSR′ ligand has long puzzled (bio)chemists and spurred experimental and computational investigations. $[Cu^I(^{DMA}N_3S)(O_2^{\bullet-})]^+$ (Chart 4) was the first example from our laboratories of a relevant synthetic model involving O_2 reactivity. Cryogenic oxygenation of $[Cu^I(^{DMA}N_3S)]^+$ led to solutions of a binuclear peroxo species $[\{Cu^I(^{DMA}N_3S)\}_2(\mu\text{-}1,2\text{-}O_2^{2-})]^{2+}$ ($\nu_{Cu–O}$ = 547 cm^{-1}, $\nu_{O–O}$ = 821 cm^{-1}). However, a change to a MeTHF:trifluoroethanol solvent at −135 °C stabilized the superoxo complex $[Cu^{II}(^{DMA}N_3S)(O_2{\bullet-})]^+$ ($\nu_{Cu–O}$ = 460 cm^{-1}, $\nu_{O–O}$ = 1117 cm^{-1}). Reactivity studies revealed that $[Cu^{II}(^{DMA}N_3S)\text{-}(O_2^{\bullet-})]^+$, with its weaker thioether donation to copper(II) as compared to complexes with N_4 ligation, could affect HAA from *p*-OMe-DTBP and *N*-methyl-9,10-dihydroacridine, whereas $[Cu^{II}(^{DMA}tmpa)(O_2^{\bullet-})]^+$ is unable to react (Figure 15).[50]

The study of the N_3S-containing complex $[Cu^{II}(^{TMG}N_3S)(O_2^{\bullet-})]^+$ (Figure 16) provided further insights. X-ray absorption fine structure (EXAFS) spectroscopy proved $Cu–S_{thioether}$

ligation (2.55 Å). For the copper(I) precursor, $[Cu^{I}(^{TMG}N_3S)](B(C_6F_5)_4)$, $Cu^{I}–S_{thioether}$ = 2.50 Å.[3] Here also, comparison of the HAA reactivity of $[Cu^{II}(^{TMG}N_3S)\text{-}(O_2^{\bullet-})]^{+}$ vs that for the N_4 analog $[Cu^{II}(TMG_3tren)(O_2^{\bullet-})]^{+}$ gives a somewhat enhanced reactivity for the former. A deeper understanding of the role of the thioether ligand here and for copper enzymes is needed.

Castillo and co-workers[51] recently studied the low-temperature copper(I)/O_2 chemistry with the benzimidazole-containing N_3S ligand L^R, Chart 4. The superoxide complex proposed to form possesses η^2-side-on binding. A triplet ground state is implicated based on the observation of paramagnetically broadened ligand signals. $[Cu^{II}(L^R)(O_2^{\bullet-})]^{+}$ complexes were shown to oxidize dihydroanthracene to give anthraquinone.

4. N_3 OR N_2 TRIDENTATE OR BIDENTATE LIGANDS

In 1994, Fujisawa and Kitajima reported on the oxygenation of a copper(I) complex bearing the hydrotris(pyrazolyl)borate ($HB(3\text{-}^{t}Bu\text{-}5\text{-}^{i}Prpz)_3$) anionic ligand (Chart 5). The break-through X-ray structure of $[Cu^{II}(HB(3\text{-}^{t}Bu\text{-}5\text{-}^{i}Prpz)_3)O_2^{\bullet-})]$ (Figure 17) revealed (the first) side-on superoxo binding with d(O–O)=1.22 Å. A ν(O–O) stretch was observed at 1111 cm^{-1} in the IR study, and later rRaman interrogation gave ν(O–O) as 1112 cm^{-1} for the close analog complex $[Cu^{II}(HB(3\text{-Ad-}5\text{-}^{i}Prpz)_3)(O_2^{\bullet-})]$ (Ad = adamantyl).[52] Sharp ligand signals in the ^1H NMR spectra and a measured value of $\mu_{eff} \cong 0$ confirmed the complex to have a diamagnetic singlet ground state ($S = 0$) attributed to antiferromagnetic coupling between copper(II) $3d^9$ and superoxo unpaired electrons, highlighting the difference in electronic structure/bonding for side-on vs end-on superoxide–copper(II) species.

Itoh and co-workers[53] carried out important studies utilizing ^{R}PPEDC ligands (Chart 5) designed to generate cupric–superoxide species with distorted tetrahedral geometries. $[Cu^{II}(^{H}PPEDC)(O_2^{\bullet-})]^{+}$ possessed distinctive UV–vis charge transfer features and ν(O–O) = 1033 cm^{-1}. A parallel-mode EPR spectrum suggested the complex has a triplet ground state ($S = 1$), as do cupric–superoxides with TMPA-type ligands. $[Cu^{II}(^{R}PPEDC)(O_2^{\bullet-})]^{+}$ complexes effect ligand benzylic hydroxylation, chemistry which may closely model DβM biochemistry (Figure 2). While the ^{R}PPEDC (tridentate) cupric superoxides and those with TMPAs (tetradentates) share similar UV–vis charge transfer spectroscopy and $S = 1$ ground state properties, their reactivity grossly varies. $[Cu^{II}(^{H}PPEDC)(O_2^{\bullet-})]^{+}$ and phenol substrates undergo simple acid–base chemistry; reactions with phosphines lead to O-atom transfer (OAT); $[Cu^{II}(^{R}tmpa)(O_2^{\bullet-})]^{+}$ undergo HAA reactions with phenols, and they do not convert phosphines to phosphine–oxides (Figure 18). Itoh commented that the ^{R}PPEDC Cu–superoxide chemistry considerably differs from that for ligands like TMPA and TMG_3tren because of the imparted lower coordination number and differing donor atom type.

With the ligand derivative ^{H}PPMDC, Itoh and co-workers[54] showed that the corresponding cupric superoxide complex $[Cu^{II}(^{H}PPMDC)(O_2^{\bullet-})]^{+}$ facilitates an aldol-type reaction with carbonyl compound substrates and solvent molecule (acetone) through catalytic C–C bond formation. With the TMG-type ligands (Chart 5), Himmel and co-workers[55] also reported a similar aldol reactivity involving a cupric superoxide complex, e.g., $[Cu(TMGMP)(O_2^{\bullet-})]^{+}$ (Figure 19).

An important reactivity study was carried out by Tolman's group using the cupric–superoxide complex derived from the $^{i\text{Pr}}$PCA ligand.[56] [Cu^{II}($^{i\text{Pr}}$PCA)($O_2^{\bullet-}$)] is an end-on superoxide $S = 1$ complex (ν(O–O) = 1104 cm^{-1}). A mechanistic study revealed that net HAA reactions with phenols ^{X}ArOH (X = NO_2, CF_3, Cl, H, Me, ^{t}Bu, OMe, and NMe_2) divide into two groups. The reaction rate constants of [Cu^{II}($^{i\text{Pr}}$PCA)($O_2^{\bullet-}$)] toward ^{X}ArOH (X = NO_2, CF_3, Cl, H, and Me) increased with increasing electron-withdrawing character, acidity, and redox potential of phenol substrates, suggesting proton transfer is involved in the rate-determining step and thus a stepwise proton transfer/electron transfer mechanism. With electron-rich phenols (X = ^{t}Bu, OMe, and NMe_2), a negative Hammett value ($\rho = -2.5$) and decreasing k values with increasing phenol acidity and/or redox potential indicate the reaction mechanism involved concerted proton transfer- electron transfer (CPET) (or HAA).

Quite recently, Anderson and co-workers[57] devised a new (redox-active) ligand $^{t\text{Bu,Tol}}$DHP which led to a T-shaped cupric superoxide [Cu^{II}($^{t\text{Bu,Tol}}$$DHP^-$)($O_2^{\bullet-}$)], characterized by an array of spectroscopies and analyzed using DFT. Interestingly, [Cu^{II}($^{t\text{Bu,Tol}}$$DHP^-$)($O_2^{\bullet-}$)] could deformylate aldehydes or effect catalytic OAT to triphenylphosphine, all at RT. Moreover, [Cu^{II}($^{t\text{Bu,Tol}}$$DHP^-$)($O_2^{\bullet-}$)] showed catalytic behavior in oxidations of alcohol and hydrazine substrates, affording byproduct H_2O_2.

The Tolman group reported on the copper(I)/O_2 chemistry with several bidentate anionic BKI-type N_2 ligands (Chart 5). These gave rise to cryogenically stabilized cupric superoxo complexes with η^2-side-on binding. [Cu^{II}(^{R}BKI)($O_2^{\bullet-}$)] species were characterized crystallographically, spectroscopically, and with DFT calculations.[7a]

Along with the many copper–dioxygen adducts described utilizing newly designed low-coordinate ligands is the sterically encumbered peralkylated hydridacene (EMind)-substituted dipyrrin ligand.[58] Betley and co-workers could isolate the superoxo complex [Cu^{II}($^{\text{EMind}}$DP)($O_2^{\bullet-}$)]$^+$ upon exposure of [Cu^{I}($^{\text{EMind}}$DP)(N_2)]$^+$ to air. X-ray crystallography reveals the superoxo ligand to be side-on bound in this diamagnetic compound, possessing an O–O stretch at 1003 cm^{-1}. [Cu^{II}($^{\text{EMind}}$DP)($O_2^{\bullet--}$)]$^+$ could rapidly oxidize arylhydrazines, giving azoarene analogues and H_2O_2.

5. CONCLUSIONS

We have summarized, from our own works and perspectives, the synthetic bioinorganic chemistry of cupric superoxide complexes. The key take-home message is that the ligand architecture and variations define ligand–Cu^{I}/O_2 reactions and ligand–Cu^{II}($O_2^{\bullet-}$) chemical behavior. Key questions remain.

What is the true extent of reactivity of ligand–Cu^{II}($O_2^{\bullet-}$) complexes toward C–H, O–H, or N–H HAA chemistry? Can newer ligand designs enhance such oxidative chemistry? (a) In the Itoh system (Figure 18), use of a tridentate ligand affords an electrophilic pseudotetrahedral cupric–superoxide complex which effects HAA from a benzylic C–H bond (BDE ≥ 85 kcal/mol). This system is special; we ourselves have never (yet) successfully generated a cupric–superoxide complex employing a neutral tridentate ligand. Such a target goal is of interest. (b) While ligand H bonding toward copper-bound

superoxide ligands enhances C–H and O–H oxidative behavior, what are the inherent chemical/electronic structure origins? Can a ligand with H bonding to the distal (rather than proximal) superoxide O atom be studied? (c) We note that recent outlooks on the PHM/DβM mechanism suggest the involvement of an O_2-derived dicopper active intermediate.[59]

Monooxygenases most often proceed beyond $Cu^{II}(O_2^{\bullet-})$ intermediates via subsequent superoxide reduction–protonation. Fundamental insights concerning these downstream steps are needed. How basic (toward protons) is a coordinated superoxide? How, in detail and with mechanistic insights, is reduction coupled to the protonation to afford a copper (hydro)peroxide or H_2O_2 itself (e.g., in LPMOs or *p*MMOs)? Perhaps most critical is the elucidation of reductive O–O cleavage mechanisms in copper complexes and enzymes.

Ligand design and systematic variations in these synthetic bioinorganic studies represent a dominant theme of our work and that of others. Other researchers have also adapted TMPA and analogues for other copper chemistry purposes. These include application to (i) catalytic atom transfer radical polymerization (ATRP),[60] (ii) the ORR (to water or H_2O_2), e.g., in fuel cell-type applications,[61] (iii) water-oxidation chemistry,[62] (iv) supramolecular chemistry,[63] (v) redox-triggered molecular switches,[64] (vi) use of complexes having anticancer activity,[65] (vii) biological “activity-based sensing” and “bioorthoganol tracking”,[66] (viii) use of nitrosobenzene as a surrogate for a superoxo ligand, with the finding of varying ligand-Cu(II)($PhNO^{\bullet-}$) coordination structures with differing spin states[67] and (ix) confirmation of HAA mechanisms via in-depth DFT calculations of the kinetics-mechanisms for the $[Cu^{II}(^{R}tmpa)(O_2^{\bullet-})]^{+}/^{X}ArOH$ reactions (Figure 13) as well as the internal ligand benzylic C–H bond hydroxylation in Itoh’s monooxygenase model system reaction (Figure 18).[68] Such researchers also optimize their chemistry and elucidate fundamental principles through systematic ligand variation and then carry out detailed analyses of ligand–copper geometries, redox potentials, or other properties.

The study of copper(I)–dioxygen reactions will continue to be of considerable biological and abiological–chemical interest and importance.

ACKNOWLEDGMENTS

K.D.K. acknowledges the many high-quality contributions of former graduate students and postdoctoral associates. The writing of this article and recent research was supported by the USA NIH (R35GM139536).

Biographies

Bohee Kim received her Ph.D. degree in Chemistry in 2020 with Jaeheung Cho at the Daegu Gyeongbuk Institute of Science and Technology, studying new copper hydro and alkylperoxo complex syntheses and reactivity. Currently, she is a postdoctoral fellow in the Karlin lab at Johns Hopkins University (JHU), continuing copper biomimetic oxidative chemistries, with a current research focus on Fenton-type chemistry employing new copper(I) complex reactions with H_2O_2.

Kenneth D. Karlin is the Ira Remsen Professor of Chemistry at Johns Hopkins University, Baltimore, MD. His Ph.D. research was with S. J. Lippard at Columbia University.

After a NATO postdoctoral fellowship at Cambridge University (U.K.), he started his independent career at SUNY Albany, moving to JHU in 1990. He served as Editor-in-Chief of *Progress in Inorganic Chemistry* (Wiley Interscience) from 1992 to 2018. He chaired a Gordon Conference on Metals in Biology and organized other copper and/or bioinorganic international meetings, including the 1989 International Conference on Bioinorganic Chemistry. He's held advisory positions with the Society for Biological Inorganic Chemistry, the Petroleum Research Fund, and the ACS's Division of Inorganic Chemistry. He is the winner of the 2009 F. Albert Cotton Award in Synthetic Inorganic Chemistry and the 2021 Distinguished Service in the Advancement of Inorganic Chemistry. He is an elected ACS Fellow. He served as the JHU Department Chair from 2014 to 2017. His research interests include the coordination chemistry of bioinspired copper and heme/Cu systems, emphasizing syntheses and mechanistic studies involving small molecule (O_2, NO_x) activation.

REFERENCES

(1). Karlin KD; Wei N; Jung B; Kaderli S; Zuberbühler AD Kinetic, Thermodynamic and Spectral Characterization of the Primary Cu-O_2 Adduct in a Reversibly Formed and Structurally Characterized Peroxo-Dicopper(II) Complex. J. Am. Chem. Soc 1991, 113, 5868–5870.Our first report on the low-temperature stopped-flow UV–vis observation of $[Cu^{II}(tmpa)(O_2\bullet-)]^+$, formed on the millisecond time scale.

(2). Diaz DE; Quist DA; Herzog AE; Schaefer AW; Kipouros I; Bhadra M; Solomon EI; Karlin KD Impact of Intramolecular Hydrogen Bonding on the Reactivity of Cupric Superoxide Complexes with O–H and C–H Substrates. Angew. Chem., Int. Ed. Engl 2019, 58, 17572–17576. [PubMed: 31469942] Synthesis of cupric superoxide complexes using TMPA-type ligands possessing hydrogen-bonding groups, their characterization, and survey of their substrate hydrogen-atom abstraction (HAA) reactivity as a function of the H-bonding proficiency.

(3). Bhadra M; Transue WJ; Lim H; Cowley RE; Lee JYC; Siegler MA; Josephs P; Henkel G; Lerch M; Schindler S; Neuba A; Hodgson KO; Hedman B; Solomon EI; Karlin KD A Thioether-Ligated Cupric Superoxide Model with Hydrogen Atom Abstraction Reactivity. J. Am. Chem. Soc 2021, 143, 3707–3713. [PubMed: 33684290] Our most recent description of the ligand–copper(I)/O_2 reactivity employing a newer $N_3S_{thioether}$ ligand.

(4). Wikström M; Krab K; Sharma V Oxygen Activation and Energy Conservation by Cytochrome c Oxidase. Chem. Rev 2018, 118, 2469–2490. [PubMed: 29350917]

(5). (a)In Copper-Oxygen Chemistry; Karlin KD, Itoh S, Ed.; John Wiley & Sons, Inc.: Hoboken, NJ, 2011.(b)Lee JY, Karlin KD Elaboration of copper–oxygen mediated C–H activation chemistry in consideration of future fuel and feedstock generation. Curr. Opin. Chem. Biol 2015, 25, 184–193. [PubMed: 25756327]

(6). Meyerstein D Re-examining Fenton and Fenton-like reactions. Nat. Rev. Chem 2021, 5, 595–597. [PubMed: 37118415]

(7). (a)Elwell CE; Gagnon NL; Neisen BD; Dhar D; Spaeth AD; Yee GM; Tolman WB Copper–Oxygen Complexes Revisited: Structures, Spectroscopy, and Reactivity. Chem. Rev 2017, 117, 2059–2107. [PubMed: 28103018] (b)Quist DA; Diaz DE; Liu JJ; Karlin KD Activation of dioxygen by copper metalloproteins and insights from model complexes. J. Biol. Inorg. Chem 2017, 22, 253–288. [PubMed: 27921179]

(8). Solomon EI; Heppner DE; Johnston EM; Ginsbach JW; Cirera J; Qayyum M; Kieber-Emmons MT; Kjaergaard CH; Hadt RG; Tian L Copper Active Sites in Biology. Chem. Rev 2014, 114. 3659–3853. [PubMed: 24588098]

(9). (a)Karlin KD; Kaderli S; Zuberbühler AD Kinetics and Thermodynamics of Copper(I)/Dioxygen Interaction. Acc. Chem. Res 1997, 30, 139–147.(b)Liu JJ; Diaz DE; Quist DA; Karlin KD Copper(I)-Dioxygen Adducts and Copper Enzyme Mechanisms. Isr. J. Chem 2016, 56, 738–755.

(10). Srnec M; Navrátil R; Andris E; Jašík J; Roithová J Experimentally Calibrated Analysis of the Electronic Structure of CuO^+: Implications for Reactivity. Angew. Chem., Int. Ed. Engl 2018, 57, 17053–17057. [PubMed: 30427565]

(11). Kim B; Brueggemeyer MT; Transue WJ; Park Y; Cho J; Siegler MA; Solomon EI; Karlin KD Fenton-like Chemistry by a Copper(I) Complex and H_2O_2 Relevant to Enzyme Peroxygenase C–H Hydroxylation. J. Am. Chem. Soc 2023, 145, 11735–11744. [PubMed: 37195014]

(12). (a)Prigge ST; Eipper B; Mains R; Amzel LM Dioxygen Binds End-On to Mononuclear Copper in a Precatalytic Enzyme Complex. Science 2004, 304, 864–867. [PubMed: 15131304] (b)Klinman JP The Copper-Enzyme Family of Dopamine beta-Monooxygenase and Peptidylglycine alpha-Hydroxylating Monooxygenase: Resolving the Chemical Pathway for Substrate Hydroxylation. J. Biol. Chem 2006, 281, 3013–3016. [PubMed: 16301310]

(13). (a)Hangasky JA; Iavarone AT; Marletta MA Reactivity of O_2 versus H_2O_2 with polysaccharide monooxygenases. Proc. Natl. Acad. Sci. U. S. A 2018, 115, 4915. [PubMed: 29686097] (b)Walton PH; Davies GJ; Diaz DE; Franco-Cairo JP The histidine brace: nature's copper alternative to haem? FEBS Lett. 2023, 597, 485–494. [PubMed: 36660911]

(14). Cutsail GE; Ross MO; Rosenzweig AC; DeBeer S Towards a unified understanding of the copper sites in particulate methane monooxygenase: an X-ray absorption spectroscopic investigation. Chem. Sci 2021, 12, 6194–6209. [PubMed: 33996018]

(15). (a)Appel MJ; Meier KK; Lafrance-Vanasse J; Lim H; Tsai C-L; Hedman B; Hodgson KO; Tainer JA; Solomon EI; Bertozzi CR Formylglycine-generating enzyme binds substrate directly at a mononuclear Cu(I) center to initiate O_2 activation. Proc. Natl. Acad. Sci. U. S. A 2019, 116, 5370–5375. [PubMed: 30824597] (b)Wu Y; Zhao C; Su Y; Shaik S; Lai W Mechanistic Insight into Peptidyl-Cysteine Oxidation by the Copper-Dependent Formylglycine-Generating Enzyme. Angew Chem., Int. Ed. Engl 2023, 62, No. e202212053. [PubMed: 36545867]

(16). Rokhsana D; Shepard EM; Brown DE; Dooley DM Amine Oxidase and Galactose Oxidase. In Copper-Oxygen Chemistry; Itoh S, Karlin KD, Ed.; John Wiley & Sons, Inc.: Hoboken, NJ, 2011; Vol. 4, Chapter 3, pp 53–106.

(17). (a)Sheng Y; Abreu IA; Cabelli DE; Maroney MJ; Miller A-F; Teixeira M; Valentine JS Superoxide Dismutases and Superoxide Reductases. Chem. Rev 2014, 114, 3854–3918. [PubMed: 24684599] (b)Ohtsu H; Shimazaki Y; Odani A; Yamauchi O; Mori W; Itoh S; Fukuzumi S Synthesis and characterization of imidazolate-bridged dinuclear complexes as active site models of Cu. Zn-SOD. J. Am. Chem. Soc 2000, 122, 5733–5741.

(18). Adam SM; Wijeratne GB; Rogler PJ; Diaz DE; Quist DA; Liu JJ; Karlin KD Synthetic Fe/Cu Complexes: Toward Understanding Heme-Copper Oxidase Structure and Function. Chem. Rev 2018, 118, 10840–11022. [PubMed: 30372042]

(19). Holm RH; Kennepohl P; Solomon EI Structural and Functional Aspects of Metal Sites in Biology. Chem. Rev 1996, 96, 2239–2314. [PubMed: 11848828]

(20). Yoon J; Liboiron BD; Sarangi R; Hodgson KO; Hedman B; Solomon EI The two oxidized forms of the trinuclear Cu cluster in the multicopper oxidases and mechanism for the decay of the native intermediate. Proc. Natl. Acad. Sci. U. S. A 2007, 104, 13609–13614. [PubMed: 17702865]

(21). Magnus KA; Hazes B; Ton-That H; Bonaventura C; Bonaventura J; Hol WGJ Crystallographic Analysis of Oxygenated & Deoxygenated States of Arthropod Hemocyanin Shows Unusual Differences. Proteins: Struct. Funct. Genet 1994, 19, 302–309. [PubMed: 7984626]

(22). (a)Karlin KD; Hayes JC; Juen S; Hutchinson JP; Zubieta J Tetragonal vs. Trigonal Coordination in Copper(II) Complexes with Tripod Ligands: Structures and Properties of $(Cu(C_{21}H_{24}N_4)Cl)PF6$ and $(Cu(C_{18}H_{18}N_4)Cl)PF_6$. Inorg. Chem 1982, 21, 4106–4108.(b)Schatz M; Becker M; Thaler F; Hampel F; Schindler S; Jacobson RR; Tyeklár Z; Murthy NN; Ghosh P; Chen Q; Zubieta J; Karlin KD Copper(I) Complexes, Copper(I)/O_2 Reactivity, and Copper(II) Complex Adducts, with a Series of Tetradentate Tripyridylalkylamine Tripodal Ligands. Inorg. Chem 2001, 40, 2312–2322. [PubMed: 11327908]

(23). Patterson GS; Holm RH Structural and electronic effects on the polarographic half-wave potentials of copper (II) chelate complexes. Bioinorganic Chemistry 1975, 4, 257–275. [PubMed: 1125339]

(24). Zuberbühler AD Interactions of Cu(I) Complexes with Dioxygen. In Metal Ions in Biological Systems; Sigel H, Ed.; Marcel Dekker: New York, 1976; Vol. 5, pp 325–368.

(25). Rorabacher DB Electron transfer by copper centers. Chem. Rev 2004, 104, 651–697. [PubMed: 14871138]

(26). Jacobson RR; Tyeklar Z; Farooq A; Karlin KD; Liu S; Zubieta J A CU_2-O_2 Complex. Crystal Structure and Characterization of a Reversible Dioxygen Binding System. J. Am. Chem. Soc 1988, 110, 3690–3692.

(27). (a)Wei N; Murthy NN; Chen Q; Zubieta J; Karlin KD Copper(I)/Dioxygen Reactivity of Mononuclear Complexes with Pyridyl and Quinolyl Tripodal Tetradentate Ligands: Reversible Formation of Cu:O_2 = 1:1 and 2:1 Adducts. Inorg. Chem 1994, 33, 1953–1965.(b)Zhang CX; Kaderli S; Costas M; Kim E.-i.; Neuhold Y-M; Karlin KD; Zuberbuhler AD Copper(I)-Dioxygen Reactivity of $[(L)Cu^{I}]^{+}$ (L = tris(2-pyridymethyl)amine): Kinetic/Thermodynamic and Spectroscopic Studies Concerning the Formation of Cu-O_2 and Cu_2-O_2 Adducts as a Function of Solvent Medium and 4-Pyridyl Ligand Substituent Variations. Inorg. Chem 2003, 42, 1807–1824. [PubMed: 12639113]

(28). Fry HC; Scaltrito DV; Karlin KD; Meyer GJ The rate of O_2 and CO binding to a copper complex, determined by a “flash-and-trap” technique, exceeds that for hemes. J. Am. Chem. Soc 2003, 125, 11866–11871. [PubMed: 14505408]

(29). (a)Fukuzumi S; Kotani H; Lucas HR; Doi K; Suenobu T; Peterson RL; Karlin KD Mononuclear Copper Complex-Catalyzed Four-Electron Reduction of Oxygen. J. Am. Chem. Soc 2010, 132, 6874–6875. [PubMed: 20443560] (b)Kakuda S; Rolle CJ; Ohkubo K; Siegler MA; Karlin KD; Fukuzumi S Lewis Acid-Induced Change from Four- to Two-Electron Reduction of Dioxygen Catalyzed by Copper Complexes Using Scandium Triflate. J. Am. Chem. Soc 2015, 137, 3330–3337. [PubMed: 25659416]

(30). Hayashi H; Fujinami S; Nagatomo S; Ogo S; Suzuki M; Uehara A; Watanabe Y; Kitagawa T A Bis(mu-oxo)dicopper(III) Complex with Aromatic Nitrogen Donors: Structural Characterization and Reversible Conversion between Copper(I) and Bis(mu-oxo)-dicopper(III) Species. J. Am. Chem. Soc 2000, 122, 2124–2125.

(31). (a)Maiti D; Fry HC; Woertink JS; Vance MA; Solomon EI; Karlin KDA 1:1 Copper-Dioxygen Adduct is an End-on Bound Superoxo Copper(II) Complex which Undergoes Oxygenation Reactions with Phenols. J. Am. Chem. Soc 2007, 129, 264–265. [PubMed: 17212392] (b)Lee JY; Peterson RL; Ohkubo K; Garcia-Bosch I; Himes RA; Woertink J; Moore CD; Solomon EI; Fukuzumi S; Karlin KD Mechanistic Insights into the Oxidation of Substituted Phenols via Hydrogen Atom Abstraction by a Cupric–Superoxo Complex. J. Am. Chem. Soc 2014, 136, 9925–9937. [PubMed: 24953129]

(32). Würtele C; Gaoutchenova E; Harms K; Holthausen MC; Sundermeyer J; Schindler S Crystallographic Characterization of a Synthetic 1:1 End-On Copper Dioxygen Adduct Complex. Angew. Chem., Int. Ed. Engl 2006, 45, 3867–3869. [PubMed: 16671142]

(33). Lanci MP; Smirnov VV; Cramer CJ; Gauchenova EV; Sundermeyer J; Roth JP Isotopic Probing of Molecular Oxygen Activation at Copper(I) Sites. J. Am. Chem. Soc 2007, 129, 14697–14709. [PubMed: 17960903]

(34). Woertink JS; Tian L; Maiti D; Lucas HR; Himes RA; Karlin KD; Neese F; Würtele C; Holthausen MC; Bill E; Sundermeyer J; Schindler S; Solomon EI Spectroscopic and Computational Studies of an End-on Bound Superoxo-Cu(II) Complex: Geometric and Electronic Factors That Determine the Ground State. Inorg. Chem 2010, 49, 9450–9459. [PubMed: 20857998]

(35). Quek SY; Debnath S; Laxmi S; van Gastel M; Krämer T; England J Sterically Stabilized End-On Superoxocopper(II) Complexes and Mechanistic Insights into Their Reactivity with O–H, N–H, and C–H Substrates. J. Am. Chem. Soc 2021, 143, 19731–19747. [PubMed: 34783549]

(36). Davydov R; Herzog AE; Jodts RJ; Karlin KD; Hoffman BM End-On Copper(I) Superoxo and Cu(II) Peroxo and Hydroperoxo Complexes Generated by Cryoreduction/Annealing and Characterized by EPR/ENDOR Spectroscopy. J. Am. Chem. Soc 2022, 144, 377–389. [PubMed: 34981938]

(37). Wada A; Honda Y; Yamaguchi S; Nagatomo S; Kitagawa T; Jitsukawa K; Masuda H Steric and hydrogen-bonding effects on the stability of copper complexes with small molecules. Inorg. Chem 2004, 43, 5725–5735. [PubMed: 15332825]

(38). (a)Bhadra M; Lee JYC; Cowley RE; Kim S; Siegler MA; Solomon EI; Karlin KD Intramolecular Hydrogen Bonding Enhances Stability and Reactivity of Mononuclear Cupric Superoxide Complexes. J. Am. Chem. Soc 2018, 140, 9042–9045. [PubMed: 29957998] (b)Peterson RL; Himes RA; Kotani H; Suenobu T; Tian L; Siegler MA; Solomon EI; Fukuzumi S; Karlin KD Cupric Superoxo-Mediated Intermolecular C–H Activation Chemistry. J. Am. Chem. Soc 2011, 133, 1702–1705. [PubMed: 21265534]

(39). Schatz M; Raab V; Foxon SP; Brehm G; Schneider S; Reiher M; Holthausen MC; Sundermeyer J; Schindler S Combined spectroscopic and theoretical evidence for a persistent end-on copper superoxo complex. Angew. Chem., Int. Ed. Engl 2004, 43, 4360–4363. [PubMed: 15368393]

(40). Peterson RL; Ginsbach JW; Cowley RE; Qayyum MF; Himes RA; Siegler MA; Moore CD; Hedman B; Hodgson KO; Fukuzumi S; Solomon EI; Karlin KD Stepwise Protonation and Electron-Transfer Reduction of a Primary Copper–Dioxygen Adduct. J. Am. Chem. Soc 2013, 135, 16454–16467. [PubMed: 24164682]

(41). Cao R; Saracini C; Ginsbach JW; Kieber-Emmons MT; Siegler MA; Solomon EI; Fukuzumi S; Karlin KD Peroxo and Superoxo Moieties Bound to Copper Ion: Electron-Transfer Equilibrium with a Small Reorganization Energy. J. Am. Chem. Soc 2016, 138, 7055–7066. [PubMed: 27228314]

(42). Würtele C; Sander O; Lutz V; Waitz T; Tuczek F; Schindler S Aliphatic C–H Bond Oxidation of Toluene Using Copper Peroxo Complexes That Are Stable at Room Temperature. J. Am. Chem. Soc 2009, 131, 7544–7545. [PubMed: 19441813]

(43). Komiyama K; Furutachi H; Nagatomo S; Hashimoto A; Hayashi H; Fujinami S; Suzuki M; Kitagawa T Dioxygen reactivity of copper(I) complexes with tetradentate tripodal ligands having aliphatic nitrogen donors: Synthesis, structures, and properties of peroxo and superoxo complexes. Bull. Chem. Soc. Jpn 2004, 77, 59–72.

(44). Kobayashi Y; Ohkubo K; Nomura T; Kubo M; Fujieda N; Sugimoto H; Fukuzumi S; Goto K; Ogura T; Itoh S Copper(I)-Dioxygen Reactivity in a Sterically Demanding Tripodal Tetradentate tren Ligand: Formation and Reactivity of a Mononuclear Copper(II) End-On Superoxo Complex. Eur. J. Inorg. Chem 2012, 2012, 4574–4578.

(45). Comba P; Haaf C; Helmle S; Karlin KD; Pandian S; Waleska A Dioxygen Reactivity of New Bispidine-Copper Complexes. Inorg. Chem 2012, 51, 2841–2851. [PubMed: 22332786]

(46). De Leener G; Over D; Smet C; Cornut D; Porras-Gutierrez AG; López I; Douziech B; Le Poul N; Topić F; Rissanen K; Le Mest Y; Jabin I; Reinaud O Two-Story" Calix[6]arene-Based Zinc and Copper Complexes: Structure, Properties, and O_2 Binding. Inorg. Chem 2017, 56, 10971–10983. [PubMed: 28853565]

(47). Nappa M; Valentine JS; Miksztal A; Schugar HJ; Isied SS Reactions of superoxide in aprotic solvents. A superoxo complex of copper(II) rac-5,7,7,12,14,14-hexamethyl-1,4,8,11-tetraazacyclotetradecane. J. Am. Chem. Soc 1979, 101, 7744–7746.

(48). Hoppe T; Schaub S; Becker J; Würtele C; Schindler S Characterization of a Macrocyclic end-on Peroxido Copper Complex. Angew. Chem., Int. Ed. Engl 2013, 52, 870–873. [PubMed: 23180566]

(49). Gómez-Vidales V; Castillo I Thioether-Containing Copper Complexes as PHM, DβM, and TβM Model Systems. Eur. J. Inorg. Chem 2022, 2022, No. e202100728.

(50). Kim S; Lee JY; Cowley RE; Ginsbach JW; Siegler MA; Solomon EI; Karlin KD A $N_3S_{(thioether)}$-Ligated Cu^{II}-Superoxo with Enhanced Reactivity. J. Am. Chem. Soc 2015, 137, 2796–2799. [PubMed: 25697226]

(51). Sanchez-Eguia BN; Flores-Alamo M; Orio M; Castillo I Side-on cupric-superoxo triplet complexes as competent agents for H-abstraction relevant to the active site of PHM. Chem. Commun 2015, 51, 11134–11137.

(52). Chen P; Root DE; Campochiaro C; Fujisawa K; Solomon EI Spectroscopic and electronic structure studies of the diamagnetic side-on Cun-superoxo complex Cu^{II}-(O_2)[HB(3-R-5-(i)-Prpz)$_3$]: Antiferromagnetic coupling versus covalent delocalization. J. Am. Chem. Soc 2003, 125, 466–474. [PubMed: 12517160]

(53). (a)Kunishita A; Kubo M; Sugimoto H; Ogura T; Sato K; Takui T; Itoh S Mononuclear Copper(II)–Superoxo Complexes that Mimic the Structure and Reactivity of the Active Centers of PHM and DbM. J. Am. Chem. Soc 2009, 131, 2788–2789. [PubMed: 19209864] (b)Tano T; Okubo Y; Kunishita A; Kubo M; Sugimoto H; Fujieda N; Ogura T; Itoh S Redox Properties of a Mononuclear Copper(II)-Superoxide Complex. Inorg. Chem 2013, 52, 10431–10437. [PubMed: 24004030]

(54). Abe T; Hori Y; Shiota Y; Ohta T; Morimoto Y; Sugimoto H; Ogura T; Yoshizawa K; Itoh S Cupric-superoxide complex that induces a catalytic aldol reaction-type C–C bond formation. Commun. Chem 2019, 2, 12.

(55). Schön F; Biebl F; Greb L; Leingang S; Grimm-Lebsanft B; Teubner M; Buchenau S; Kaifer E; Rübhausen MA; Himmel H-J On the Metal Cooperativity in a Dinuclear Copper–Guanidine Complex for Aliphatic C–H Bond Cleavage by Dioxygen. Chem. Eur. J 2019, 25, 11257–11268. [PubMed: 31131927]

(56). Bailey WD; Dhar D; Cramblitt AC; Tolman WB Mechanistic Dichotomy in Proton-Coupled Electron-Transfer Reactions of Phenols with a Copper Superoxide Complex. J. Am. Chem. Soc 2019, 141, 5470–5480. [PubMed: 30907590]

(57). Czaikowski ME; McNeece AJ; Boyn J-N; Jesse KA; Anferov SW; Filatov AS; Mazziotti DA; Anderson JS Generation and Aerobic Oxidative Catalysis of a Cu(II) Superoxo Complex Supported by a Redox-Active Ligand. J. Am. Chem. Soc 2022, 144, 15569–15580. [PubMed: 35977083]

(58). Carsch KM; Iliescu A; McGillicuddy RD; Mason JA; Betley TA Reversible Scavenging of Dioxygen from Air by a Copper Complex. J. Am. Chem. Soc 2021, 143, 18346–18352. [PubMed: 34672573]

(59). Arias RJ; Welch EF; Blackburn NJ New structures reveal flexible dynamics between the subdomains of peptidylglycine monooxygenase. Implications for an open to closed mechanism. Protein Sci. 2023, 32, No. e4615.

(60). Kaur A; Ribelli TG; Schröder K; Matyjaszewski K; Pintauer T Properties and ATRP Activity of Copper Complexes with Substituted Tris(2-pyridylmethyl)amine-Based Ligands. Inorg. Chem 2015, 54, 1474–1486. [PubMed: 25625939]

(61). Smits NWG; van Dijk B; de Bruin I; Groeneveld SLT; Siegler MA; Hetterscheid DGH Influence of Ligand Denticity and Flexibility on the Molecular Copper Mediated Oxygen Reduction Reaction. Inorg. Chem 2020, 59, 16398–16409. [PubMed: 33108871]

(62). Koepke SJ; Light KM; VanNatta PE; Wiley KM; Kieber-Emmons MT Electrocatalytic Water Oxidation by a Homogeneous Copper Catalyst Disfavors Single-Site Mechanisms. J. Am. Chem. Soc 2017, 139, 8586–8600. [PubMed: 28558469]

(63). Bravin C; Badetti E; Licini G; Zonta C Tris(2-pyridylmethyl)amines as emerging scaffold in supramolecular chemistry. Coord. Chem. Rev 2021, 427, 213558.

(64). Canary JW Redox-triggered chiroptical molecular switches. Chem. Soc. Rev 2009, 38, 747–756. [PubMed: 19322467]

(65). Jopp M; Becker J; Becker S; Miska A; Gandin V; Marzano C; Schindler S Anticancer activity of a series of copper(II) complexes with tripodal ligands. Eur. J. Med. Chem 2017, 132, 274–281. [PubMed: 28371639]

(66). Iovan DA; Jia S; Chang CJ Inorganic Chemistry Approaches to Activity-Based Sensing: From Metal Sensors to Bioorthogonal Metal Chemistry. Inorg. Chem 2019, 58, 13546–13560. [PubMed: 31185541]

(67). Askari MS; Girard B; Murugesu M; Ottenwaelder X The two spin states of an end-on copper(II)-superoxide mimic. Chem. Comm 2011, 47, 8055–8057. [PubMed: 21681293]

(68). Wu P; Zhang J; Chen Q; Peng W; Wang B Theoretical perspective on mononuclear copper-oxygen mediated C–H and O–H activations: A comparison between biological and synthetic systems. Chin. J. Catal 2022, 43, 913–927.

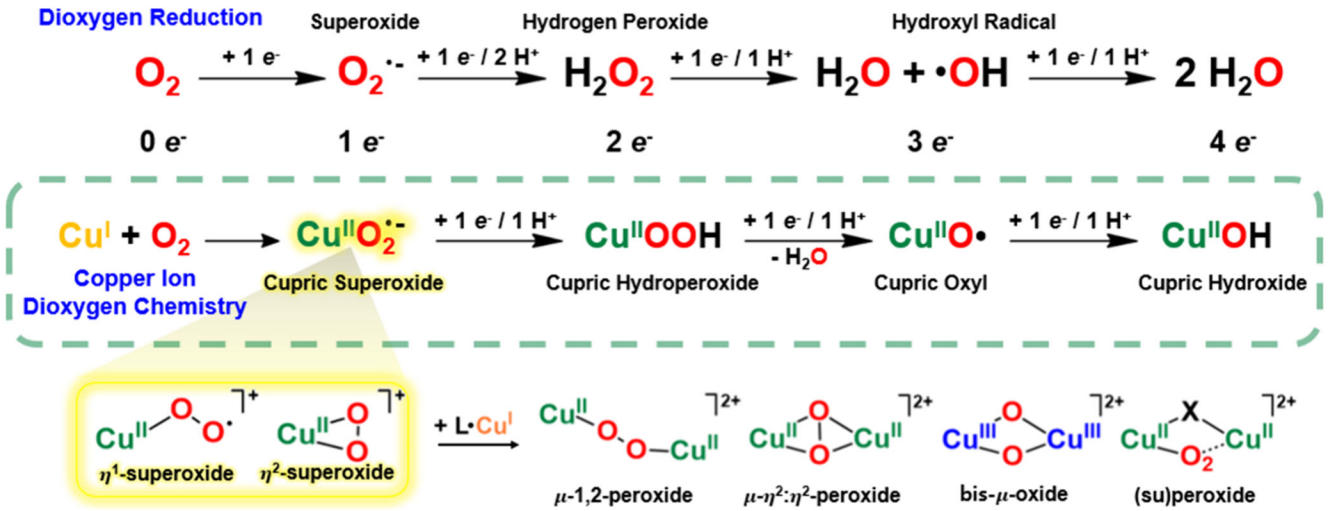

Figure 1.

Aqueous O_2 reduction chemistry, O_2 derivatives bound to copper, and reactions of cupric–superoxides giving dicopper intermediates.

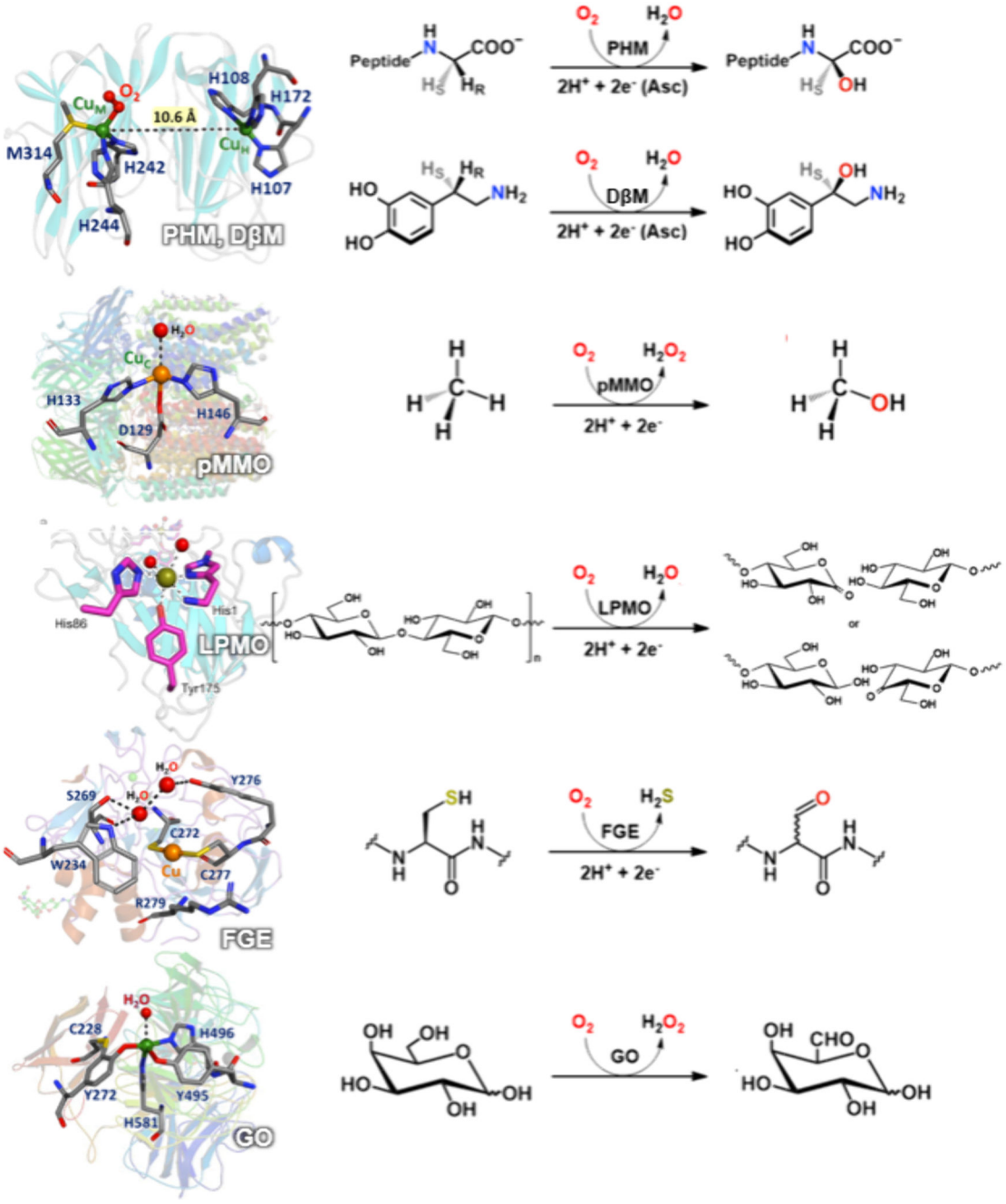

Figure 2.
Copper monooxygenase active site structures and their reactions.

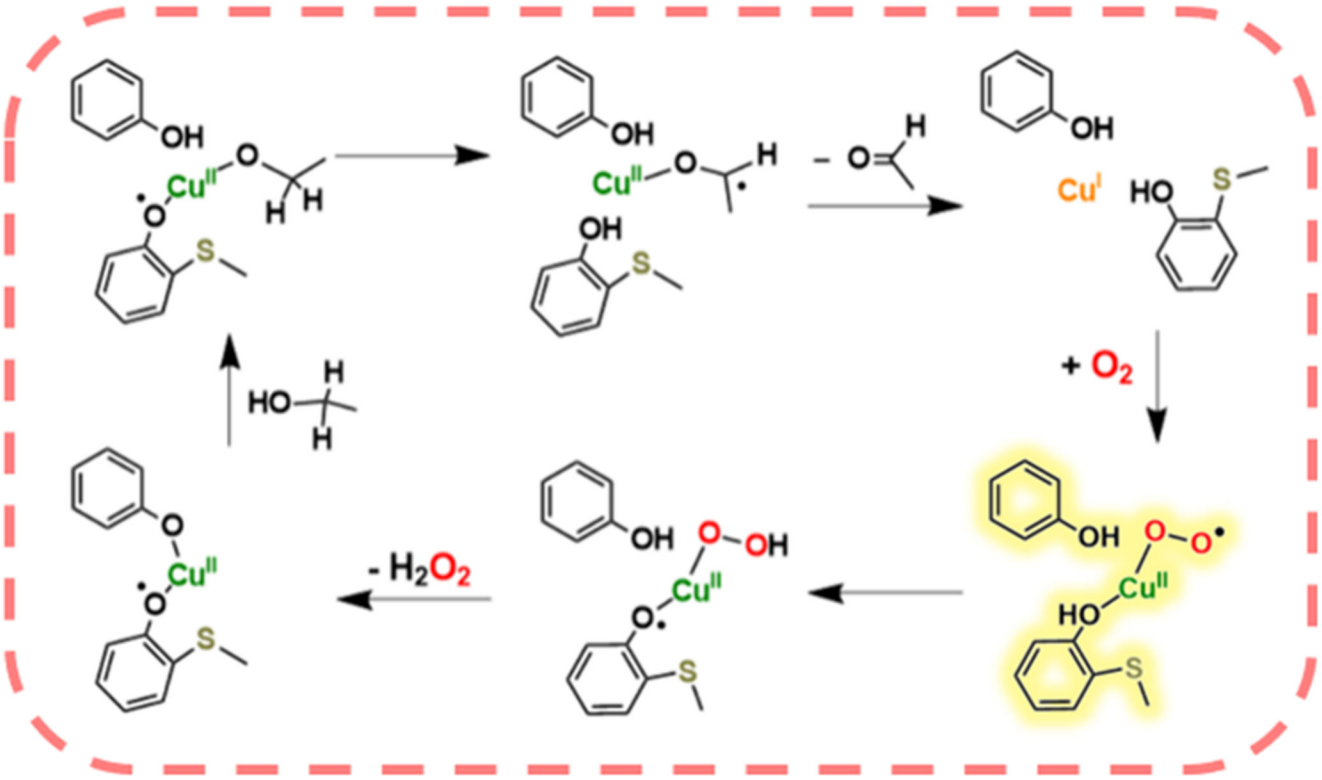

Figure 3.
GO RCH_2OH oxidation catalysis.

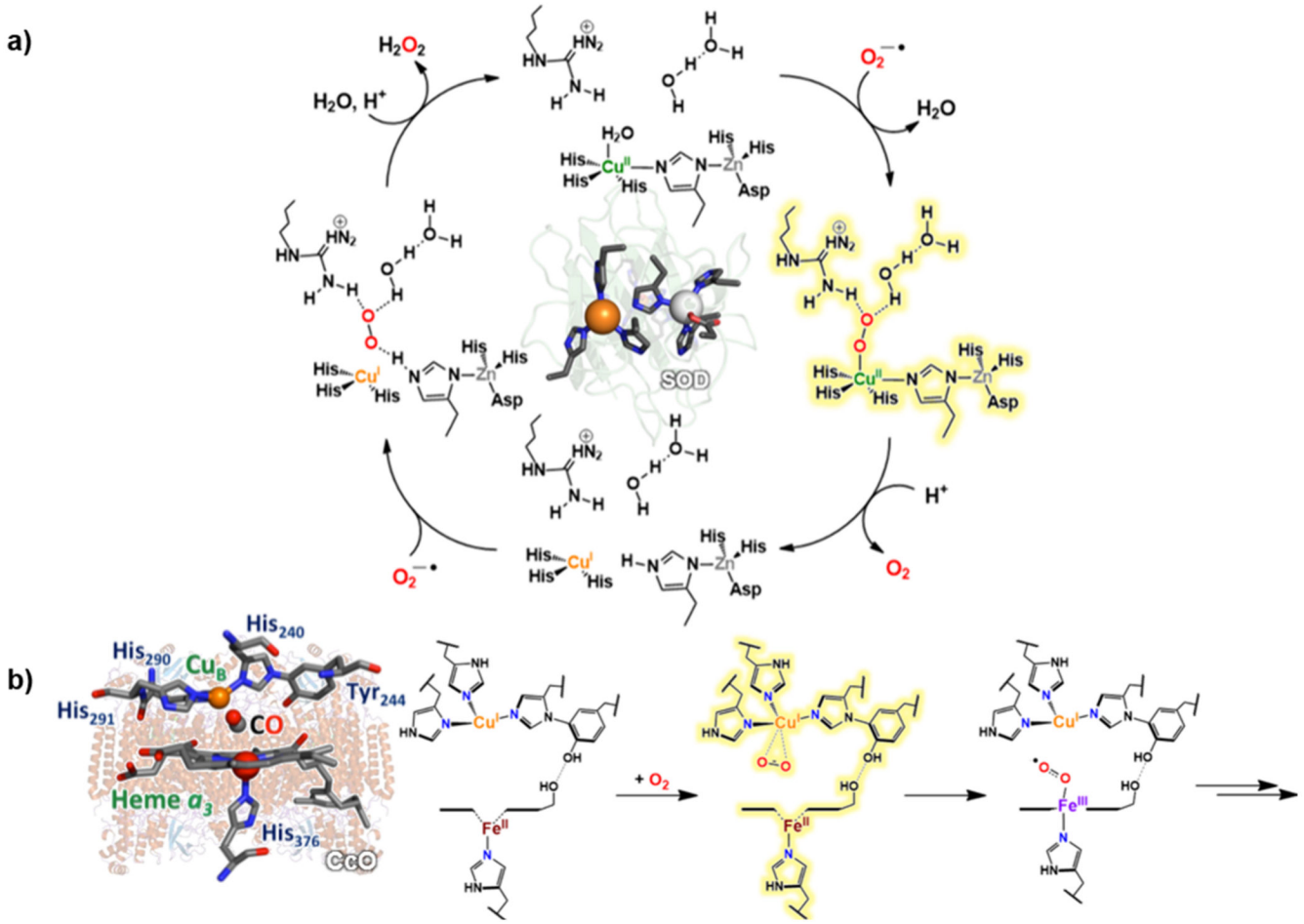

Figure 4.

(a) Mechanism of SOD1 $O_2^{\bullet-}$ disproportionation. (b) Cu^{II}–superoxide formation during O_2 addition to the reduced C*c*O heme–Cu

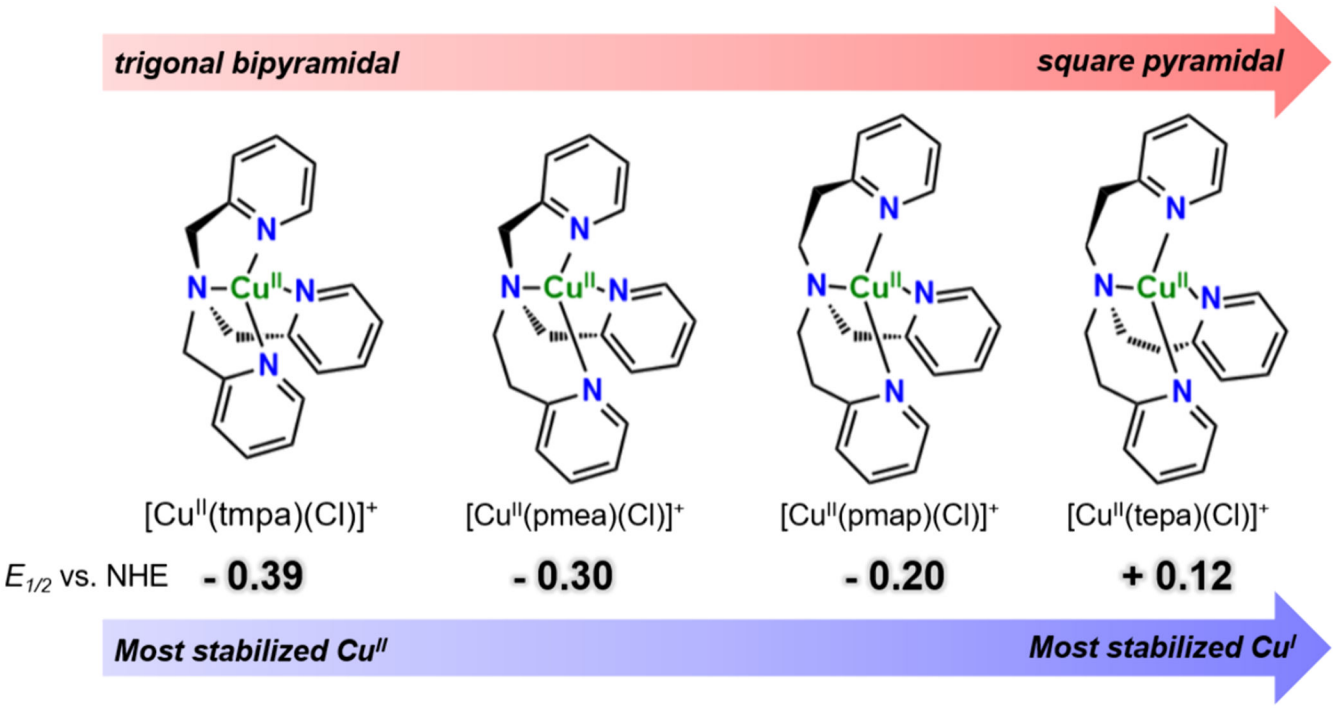

Figure 5.
Preferred geometry and redox preferences for copper(II) complexes with tripodal tetradentate ligands.

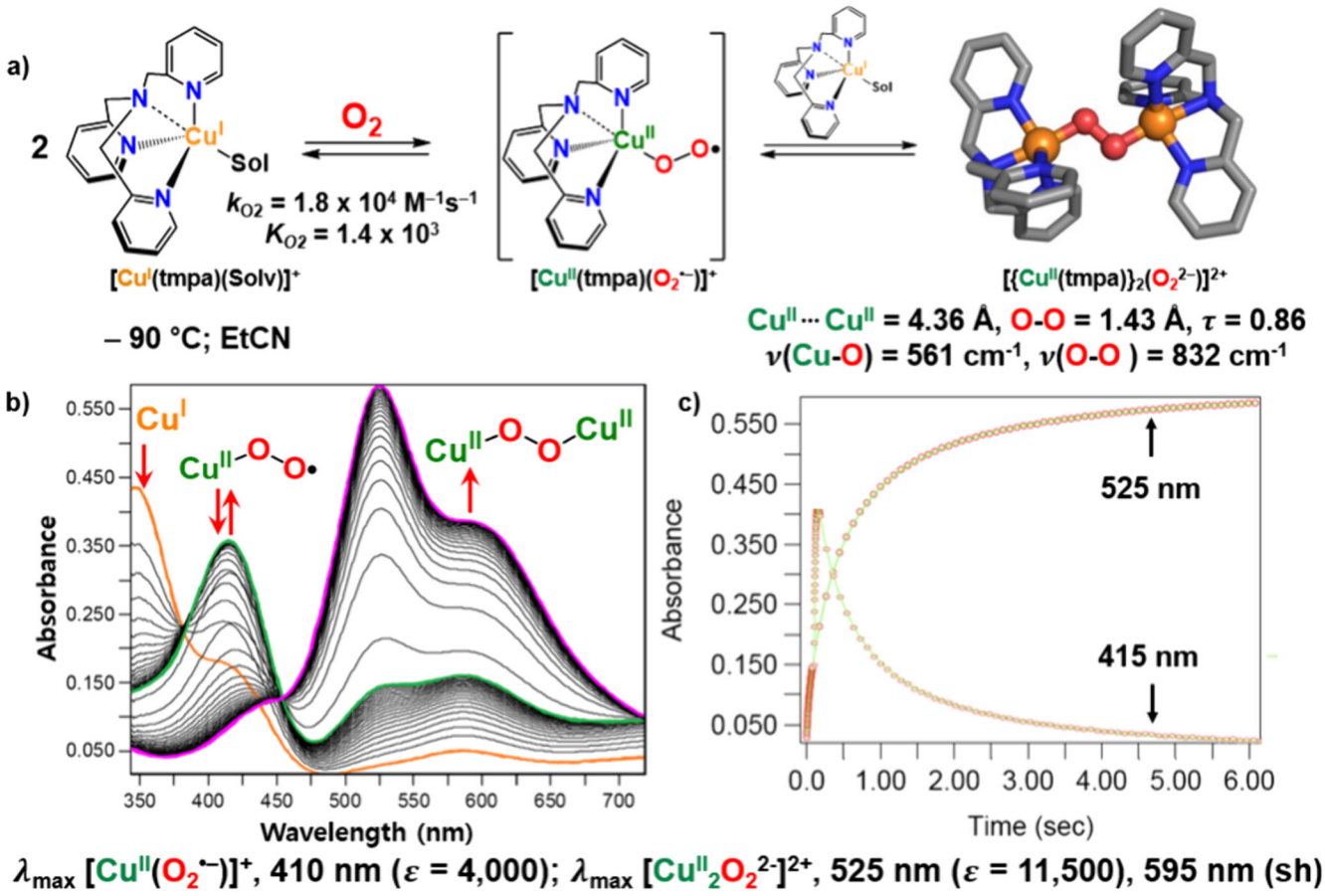

Figure 6.

(a) Oxygenation of $[Cu^{I}(tmpa)(EtCN)]^{+}$. (b) Stopped-flow UV–vis spectroscopic changes revealing the intermediacy of $[Cu^{II}(tmpa)(O_2^{\bullet-})]^{+}$ but reacts further giving $[\{Cu^{II}(tmpa)\}_2(O_2^{2-})]^{2+}$. (c) Time courses for the 415 and 525 nm absorbances.

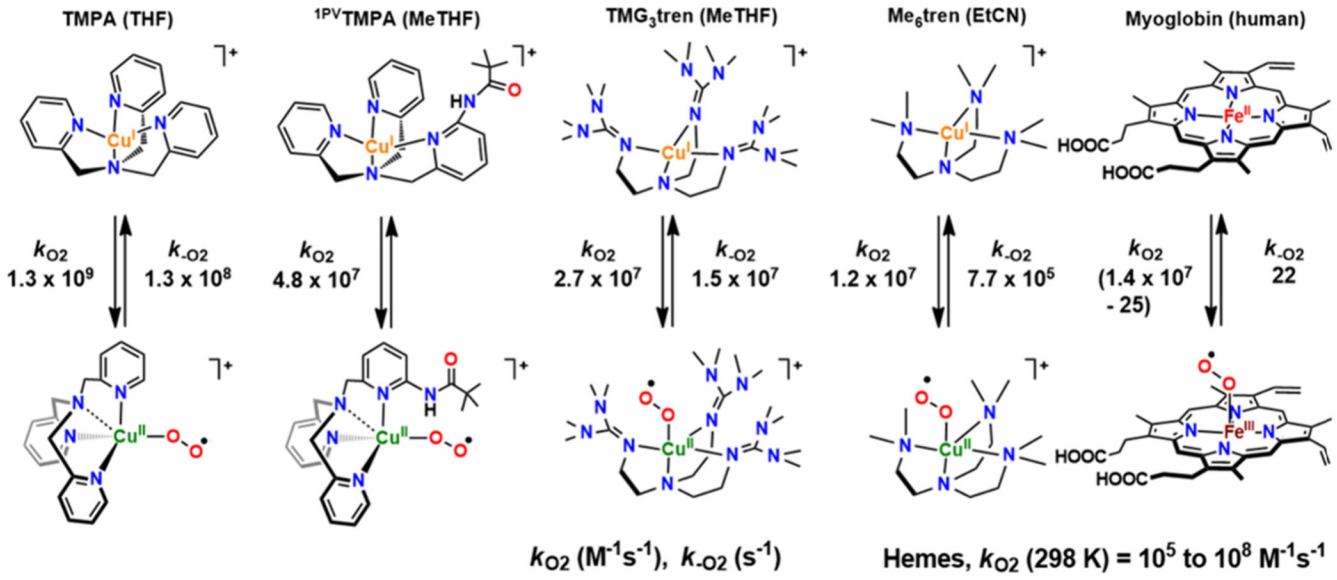

Figure 7.

Room-temperature (by extrapolation) O_2 binding rate constants for copper(I) synthetic compounds and myoglobin.[18]

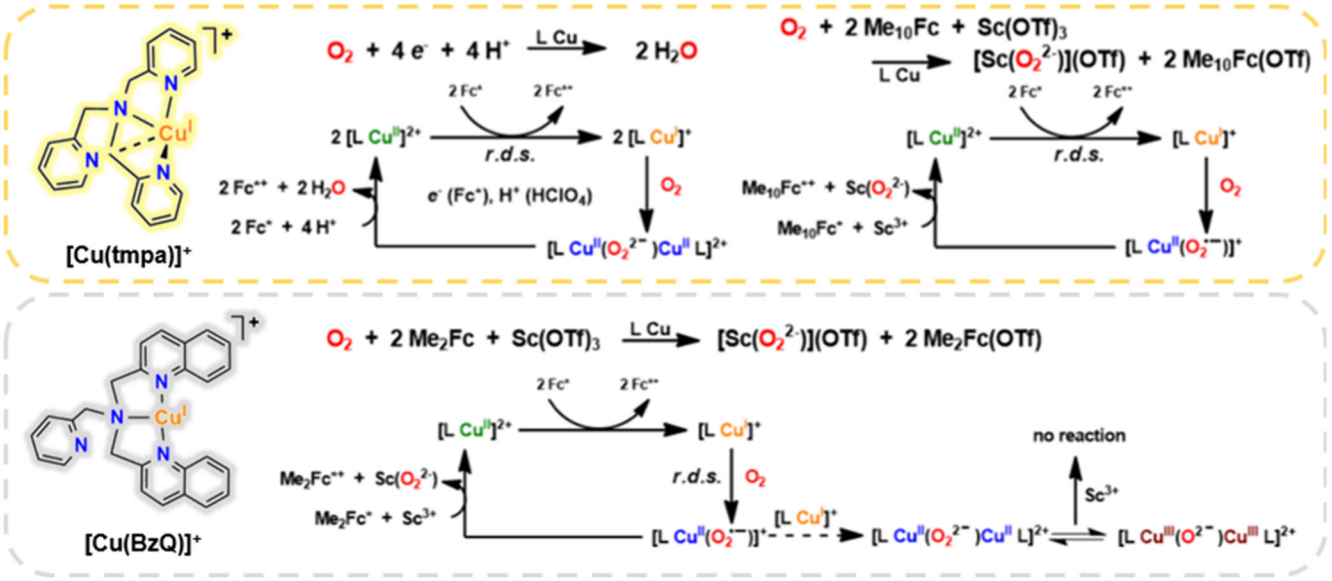

Figure 8.
ORR chemistry with $[Cu^{I}(tmpa)]^{+}$ or $[Cu^{I}(BzQ)]^{+}$.

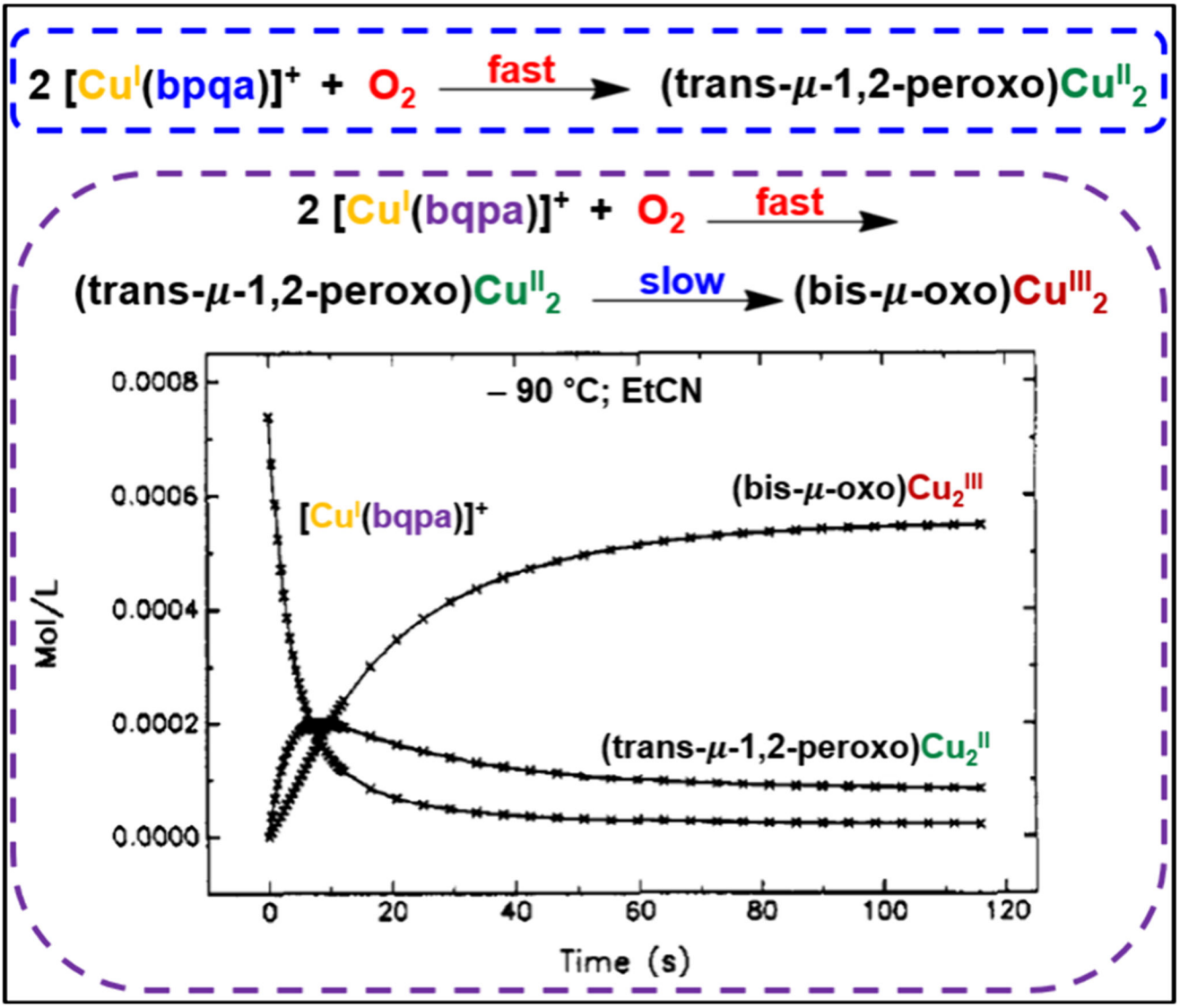

Figure 9.
$[Cu^{I}(ligand)]^{+}/O_2$ reactivity for BPQA and BQPA, and time course for $[Cu(bqpa)]^{+}/O_2$ reactivity.

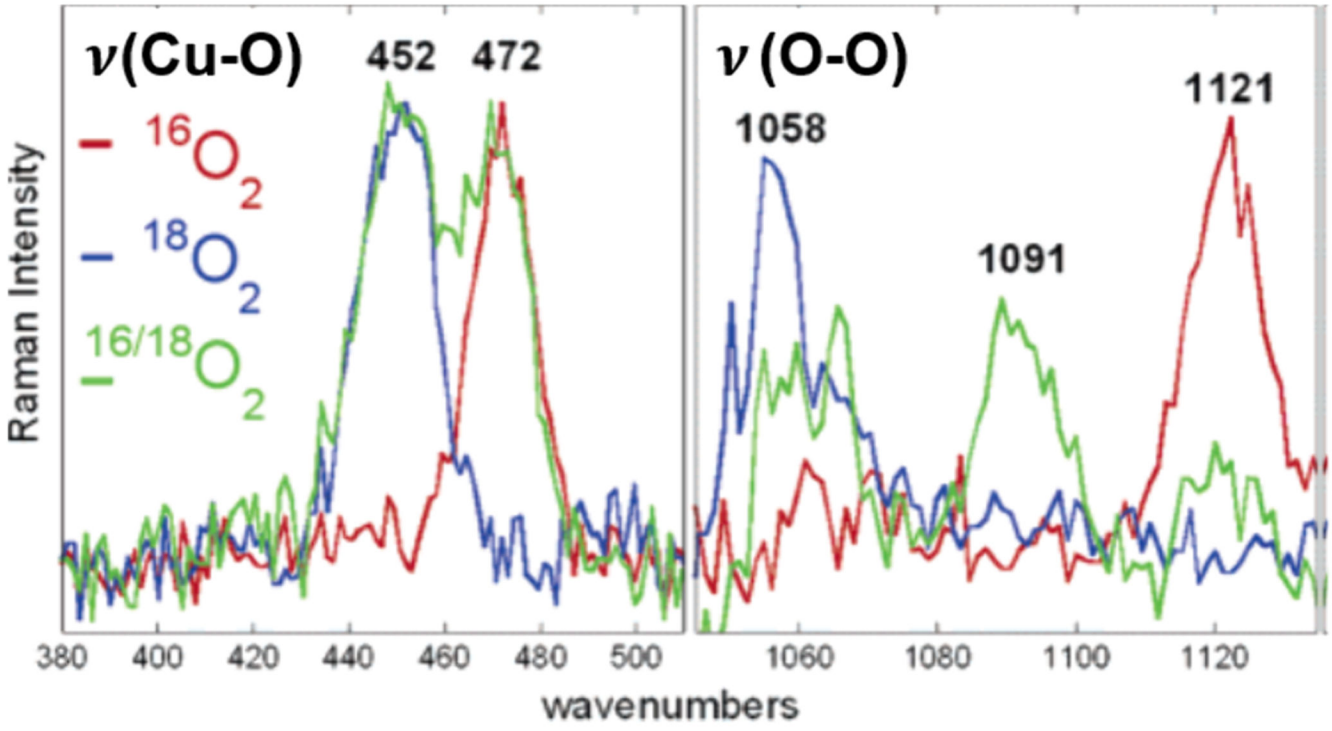

Figure 10.

Resonance Raman spectra of $[Cu^{II}(^{DMA}tmpa)(O_2^{\bullet -})]^+$ when $^{16}O_2$ (red), $^{18}O_2$ (blue), or $^{16}O_2/^{18}O_2$ (green) was utilized. Adapted with permission from ref 31a. Copyright 2007 American Chemical Society.

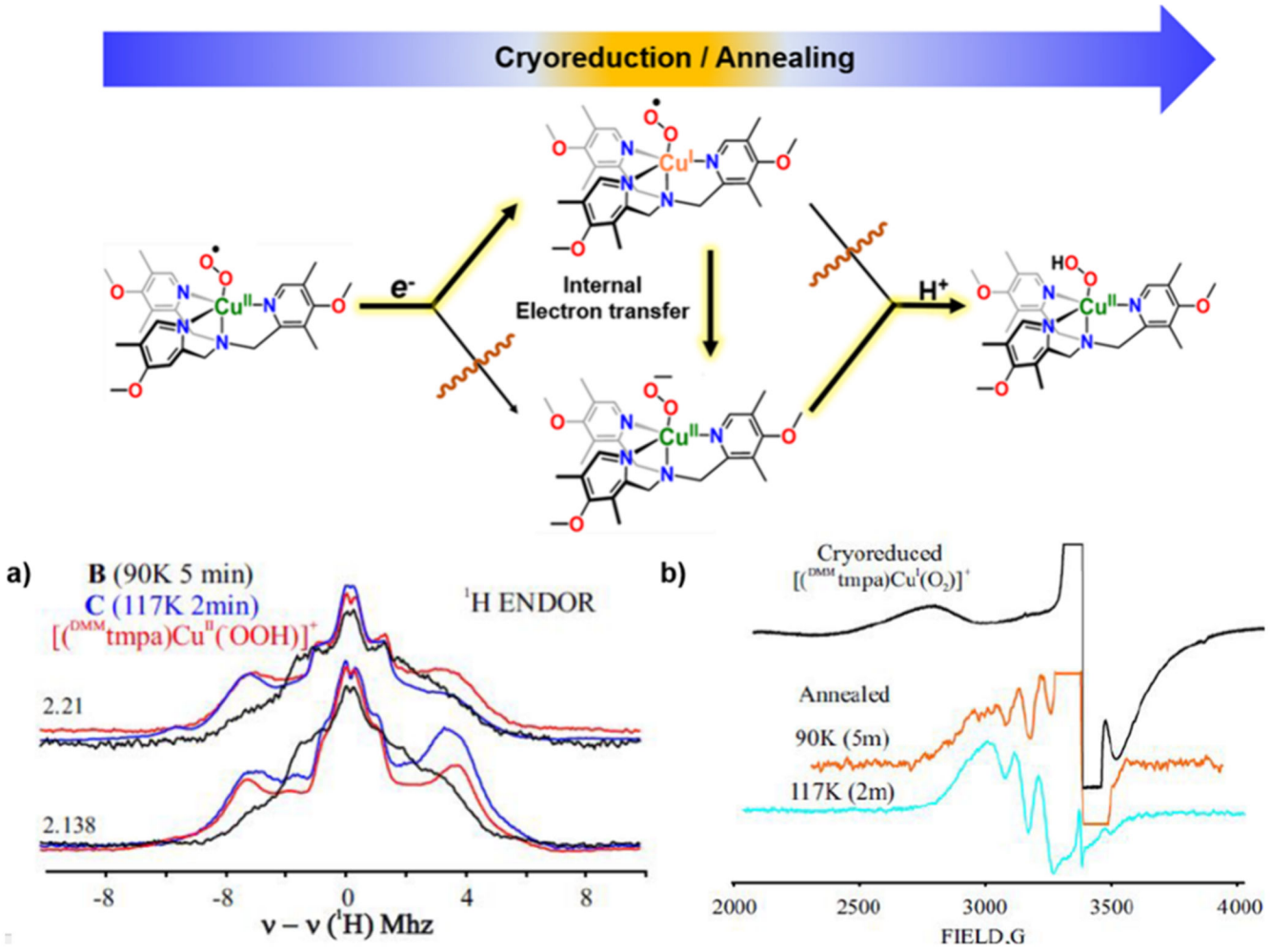

Figure 11.

Cryoreduction/annealing of $[Cu^{II}(^{DMM}tmpa)(O_2^{\bullet-})]^+$ with (a) ENDOR and (b) EPR spectroscopic monitoring. Adapted with permission from ref 36. Copyright 2022 American Chemical Society.

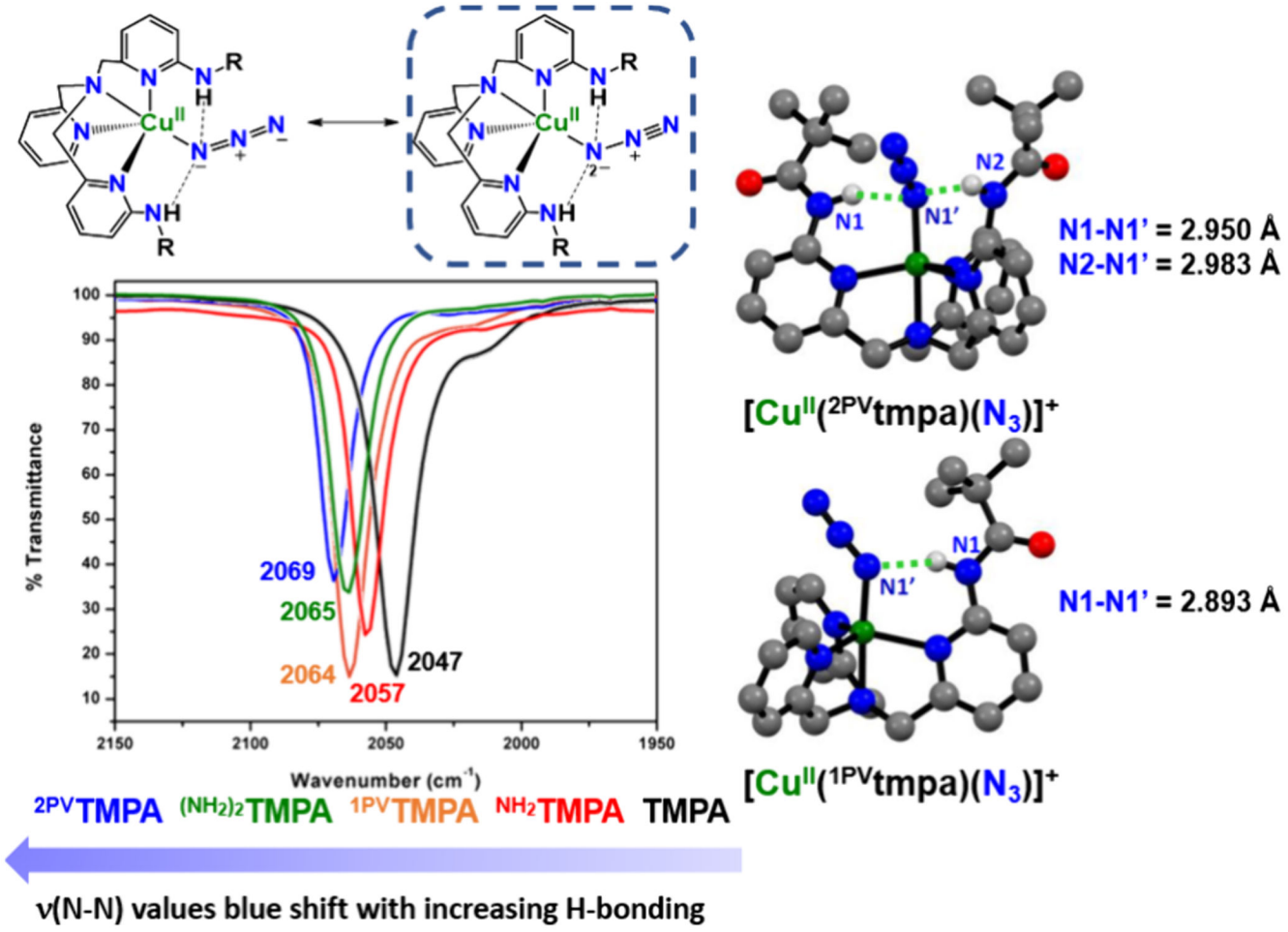

Figure 12.

Solution (CH_3CN) infrared spectra of $[Cu^{II}(^{R}tmpa)(N_3)]^+$ complexes. X-ray structures of $[Cu^{II}(^{2PV}tmpa)(N_3)]^+$ and $[Cu^{II}(^{1PV}tmpa)(N_3)]^+$.

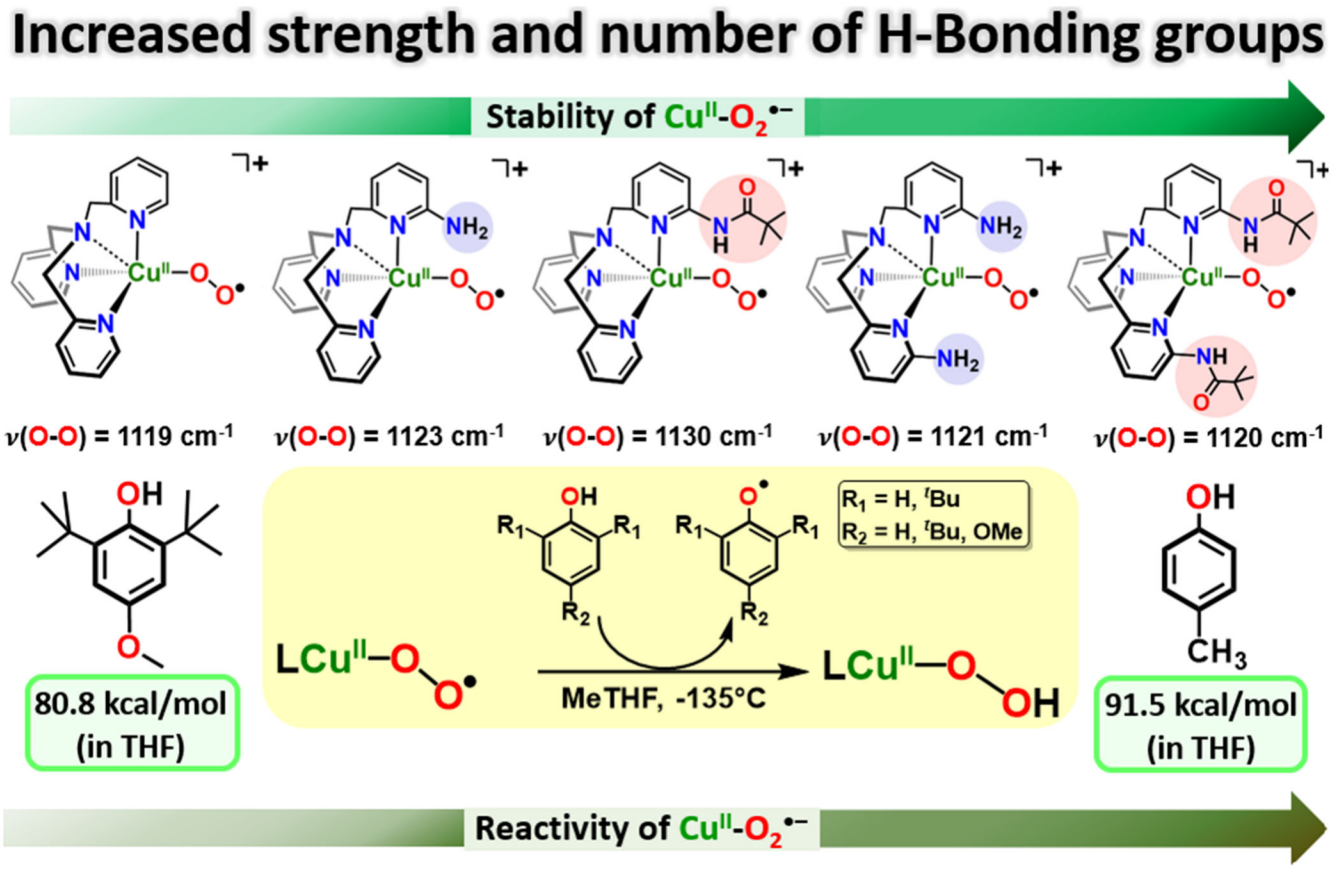

Figure 13.

Stability and reactivity of $[Cu^{II}(^{R}tmpa)(O_2^{\bullet-})]^+$ complexes as controlled by ligand hydrogen-bonding groups.

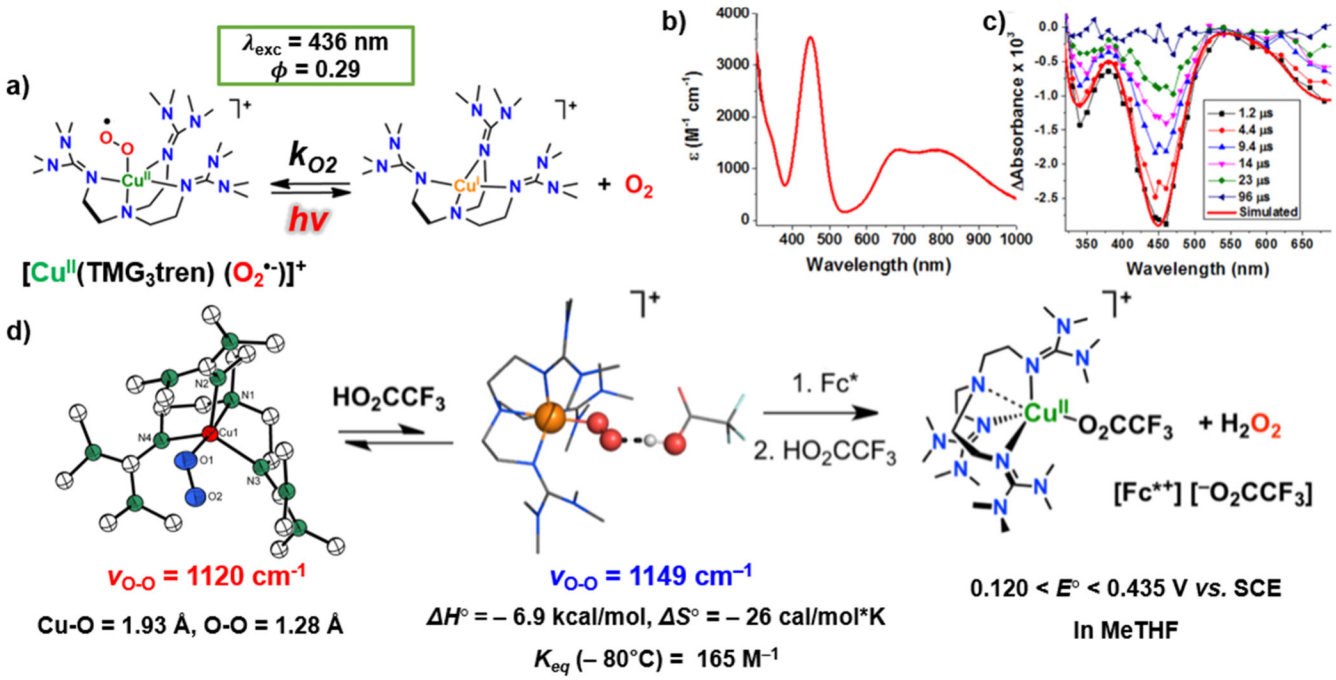

Figure 14.

(a) Superoxide–copper(II) dioxygen photoejection and rebinding to $[Cu^{I}(TMG_3tren)]^{+}$. (b) Absorption spectrum of $[Cu^{II}(TMG_3tren)(O_2^{\bullet-})]^{+}$ and (c) transient absorption (μs) difference spectra after 436 nm laser excitation. (d) The trifluoroacetic acid adduct of $[Cu^{II}(TMG_3tren)(O_2^{\bullet-})]^{+}$ and its reduction by Fc*. Adapted with permission from ref 40. Copyright 2013 American Chemical Society.

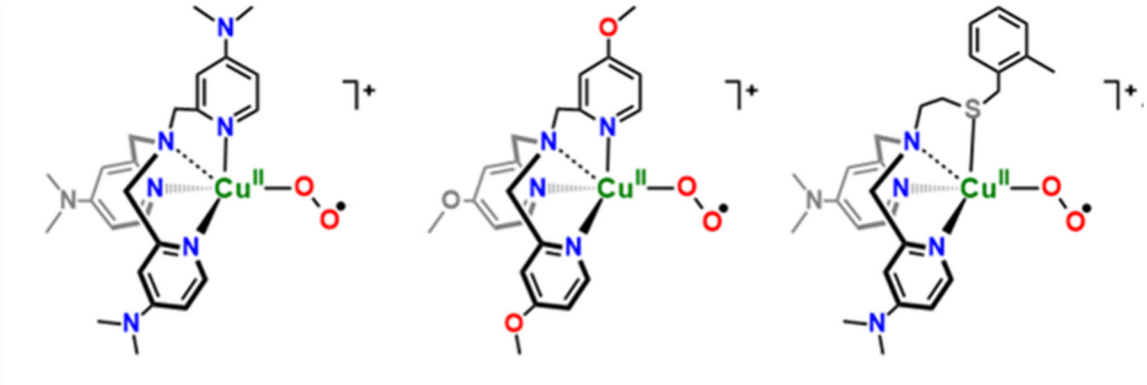

	^{DMA}TMPA	^{DMM}TMPA	$^{DMA}N_3S$
νO-O (cm^{-1})	1121	1121	1117
νCu-O (cm^{-1})	472	474	460
$E_{1/2}$ (mV)[a]	–700	–570	–470
p-OMe-DTBP	No	No	YES !
$AcrH_2$	No	No	YES !

Figure 15.
Physical properties and reactivity of selected superoxo–copper(II) complexes.

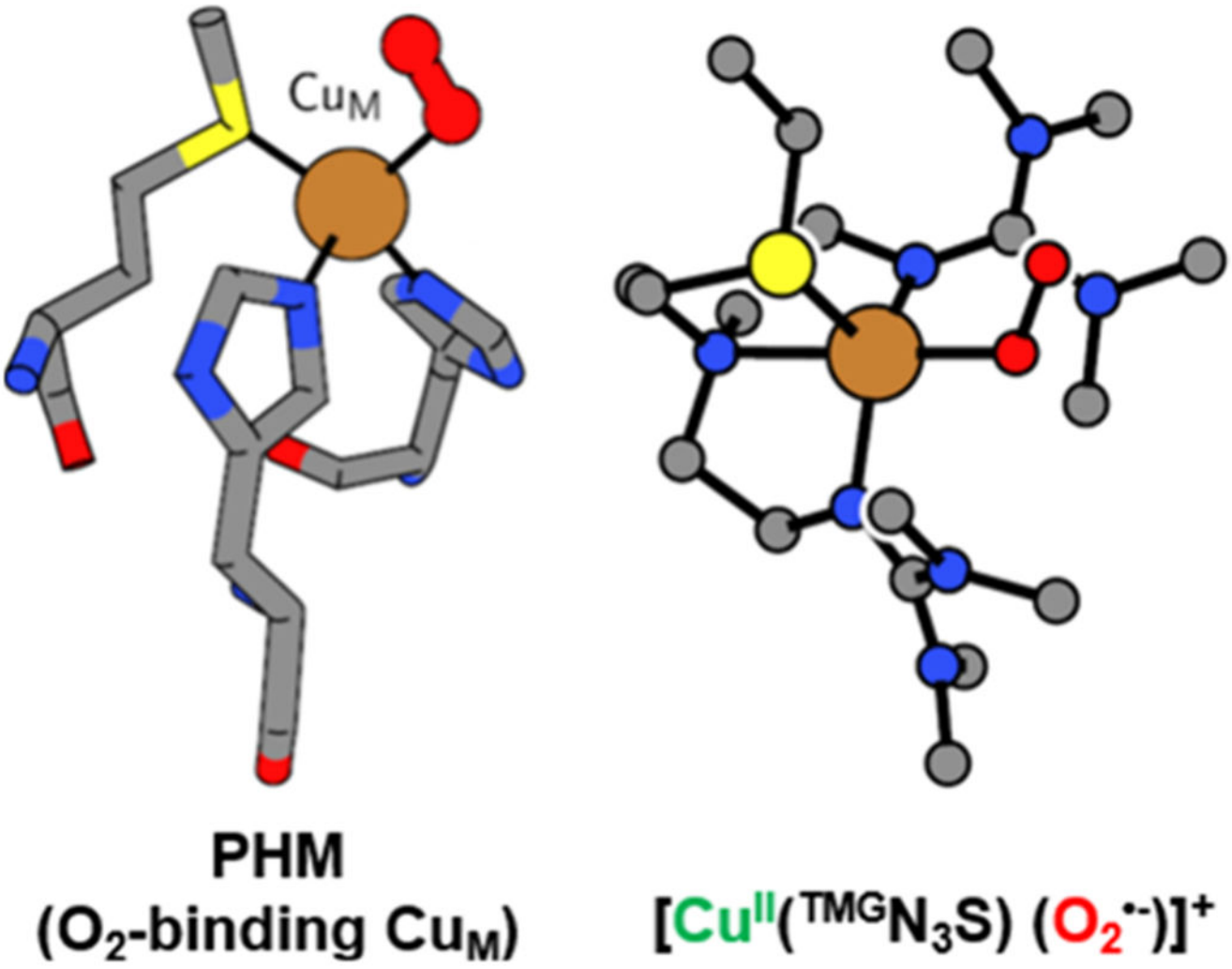

Figure 16.
Depiction of O_2-bound Cu_M in PHM and $[Cu^{II}(^{TMG}N_3S)(O_2^{\bullet-})]^+$ (ν_{O-O} = 1105 cm^{-1}). Adapted with permission from ref 3. Copyright 2021 American Chemical Society.

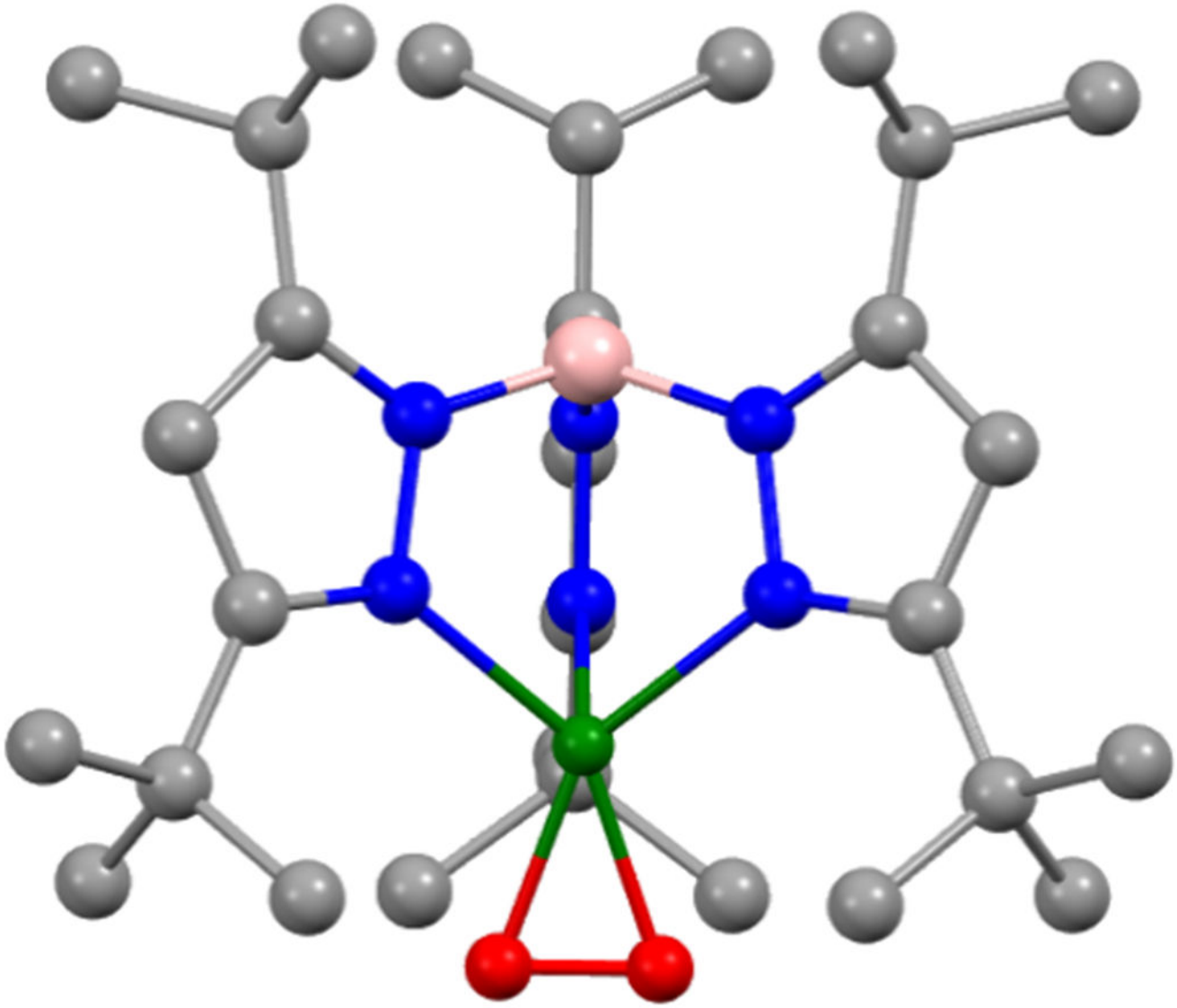

Figure 17.
Depiction of the X-ray structure of [Cu^{II}(HB(3-^{t}Bu-^{5}-^{i}PrPz)$_3$)($O_2^{\bullet-}$)].

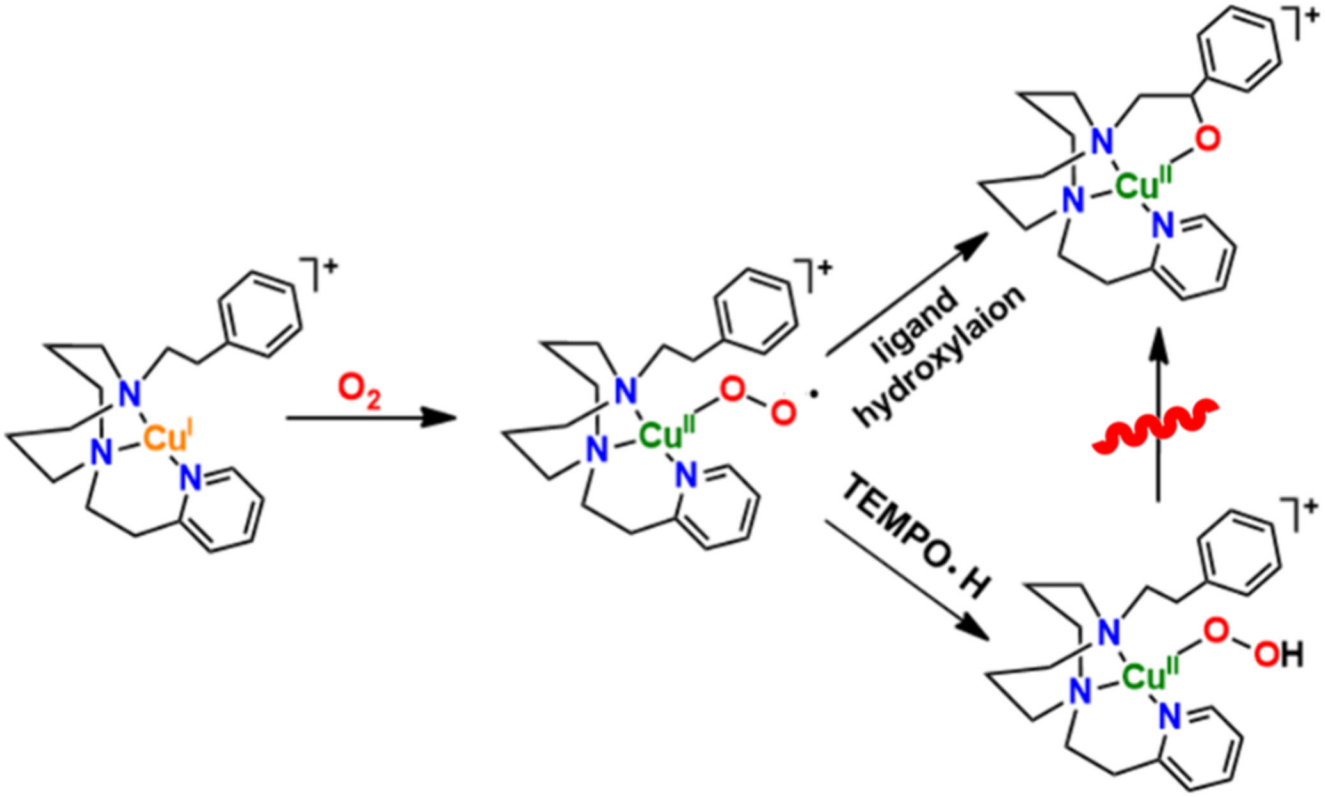

Figure 18.
Reaction pathway of $[Cu^{I}(^{H}PPEDC)]^{+}$ plus O_2 and/or TEMPO–H.

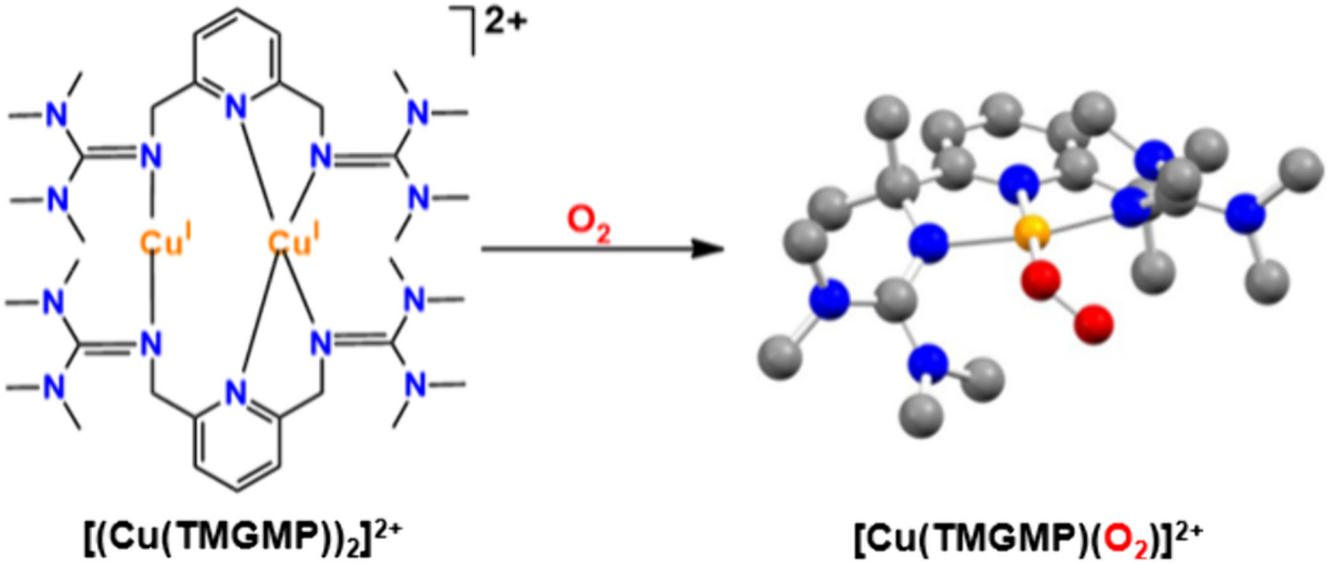

Figure 19.
A cupric–superoxide complex with the TMGMP ligand. Adapted with permission from ref 55. Copyright 2019 Wiley-VCH.

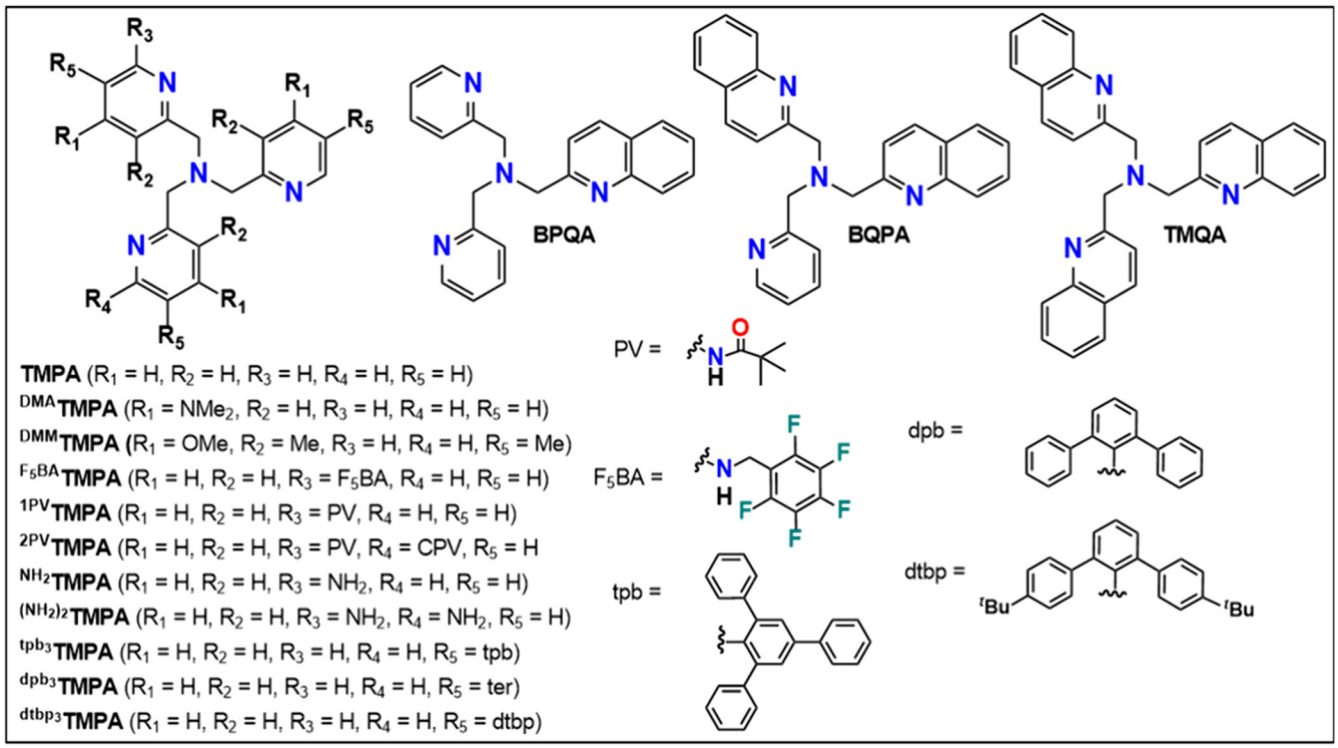

Chart 1.
N_4 Pyridylalkylamine Ligands

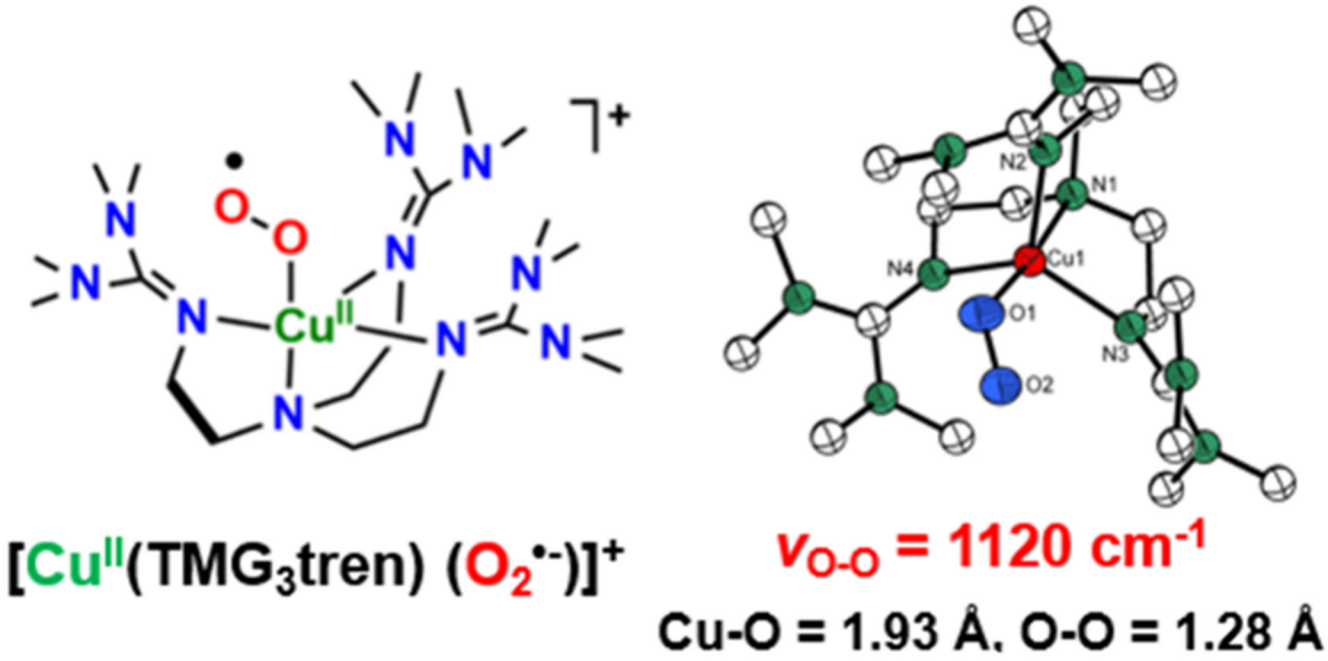

Chart 2.
Structural Representation of $[Cu^{II}(TMG_3tren)(O_2^{\bullet -})]^+$

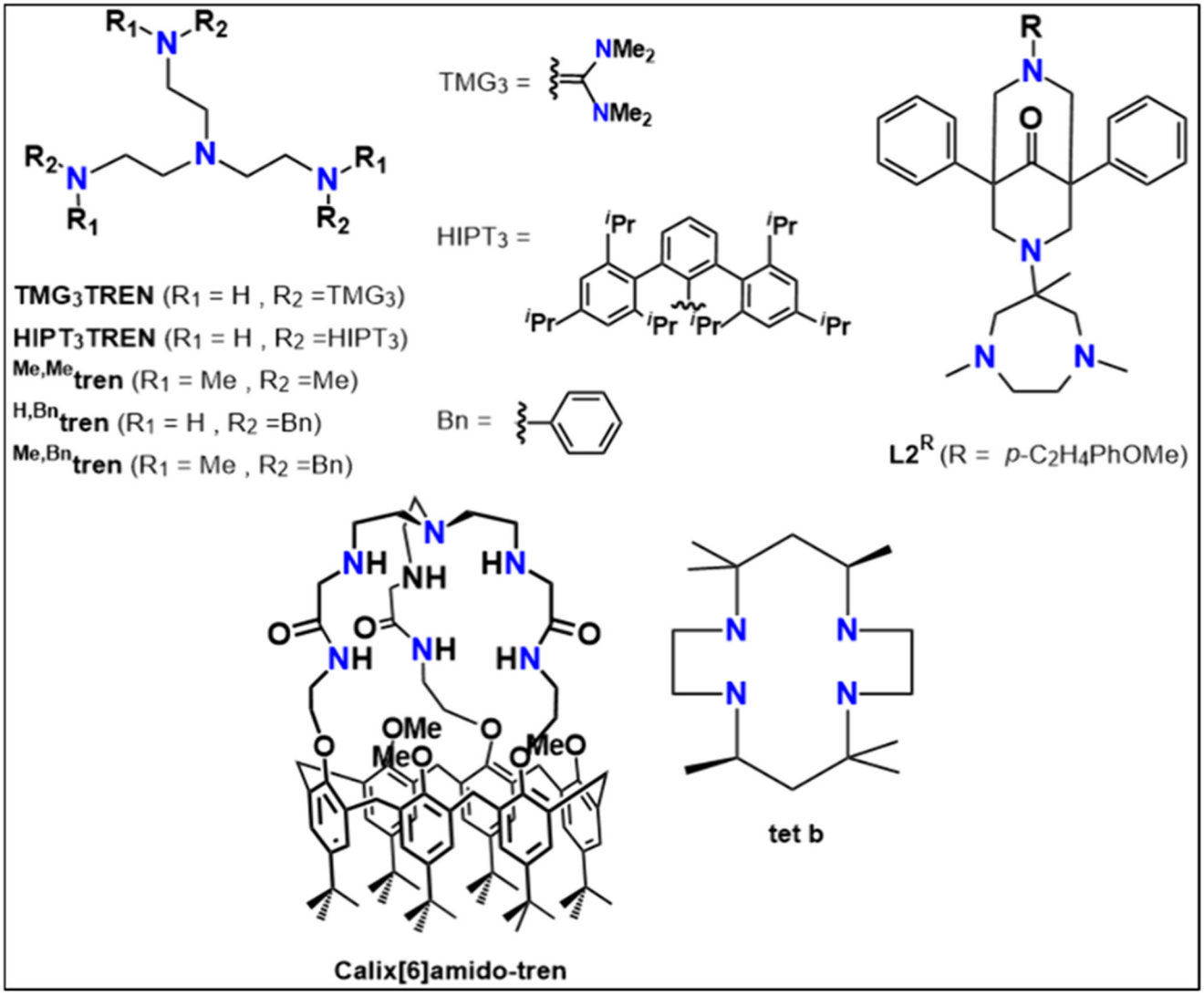

Chart 3.
N_4 tren-Type Ligands

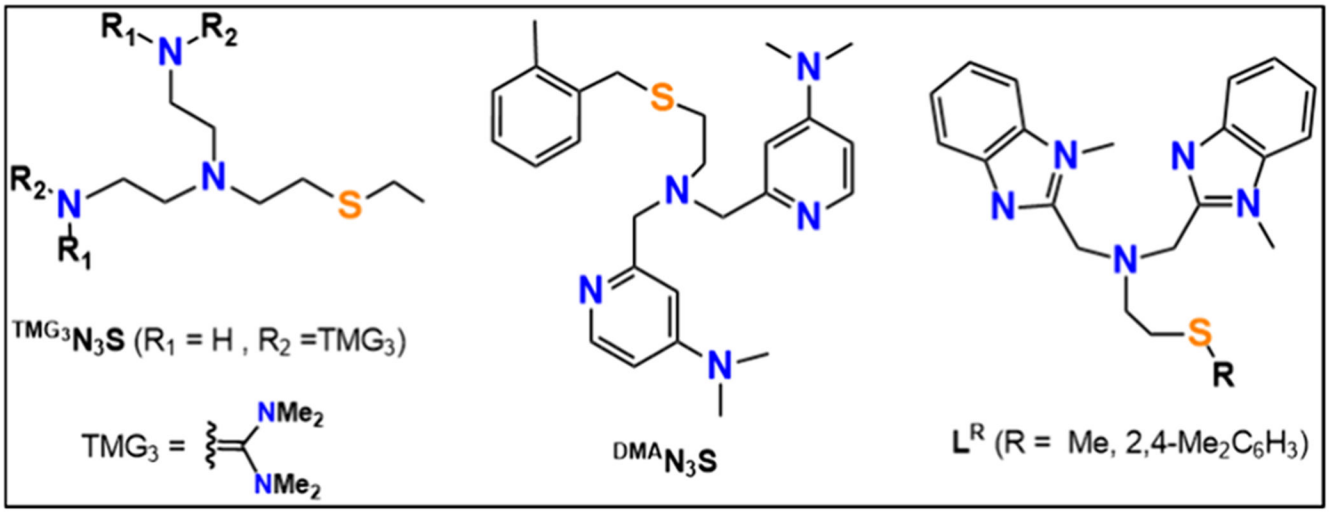

Chart 4.
N_3S Tetradentate Ligands

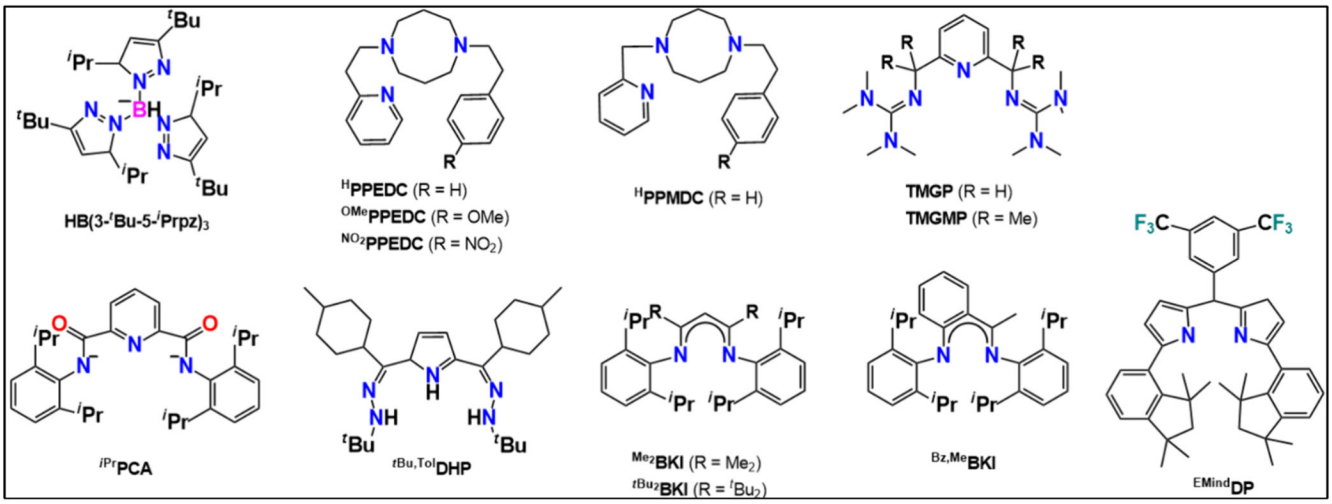

Chart 5.

N_3 or N_2 Tridentate or Bidentate Ligands

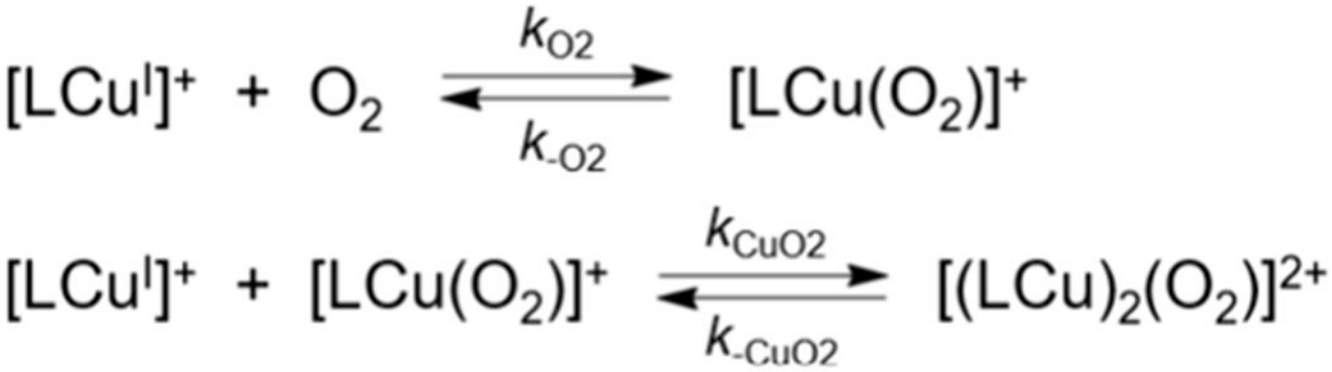

Scheme 1.
Kinetic Scheme Pertaining to Cu^{II}–Superoxo and Then Binuclear Peroxo–Dicopper(II) Complexes